Dear Editor,

Following the suggestion of the three referees we have done major modifications of the manuscript entitled “Two superimposed cold and fresh anomalies enhanced Irminger Sea deep convection in 2016–2018”.

The major changes made to the manuscript are the following.

1. The method used to define the MLD has been revised. We adapted our threshold method to include temperature and salinity criteria in addition to density criteria. We describe the revised method, indicating clearly the density, temperature and salinity threshold used. In the supplementary material, we provide a comparison of our estimates of MLDs with those obtained using other methods (de Jong et al., 2012 or Pickart et al., 2003) and show a good agreement between all these methods.
2. We included in the manuscript a computation of the percentage of floats showing deep convection in the box southeast of Cape Farewell. It varies between 33% and 75% depending on the winter.
3. The name of the studied region was changed to Southeast of Cape Farewell (SECF) instead of Irminger Sea.
4. All the terms of both atmospheric forcing (air-sea fluxes and the Ekman transport) and preconditioning (B, B_θ and B_s) have been recalculated because we changed the northern limit of the box enclosing the SECF region.

These modifications did not change the main conclusions of the study, but some results were modified as follows.

1. Using the revised method to define the MLD, the number of profiles showing deep mixed layer is smaller than in the previous version of the manuscript for all the 2016-2018 winters studied in the paper but still substantial enough to affirm that deep convection happened Southeast of Cape Farewell during those winters.
2. The new results of atmospheric forcing and preconditioning are very similar to those reported in the previous version of the manuscript.
3. Figures have been slightly modified:
   -) Fig. 1, Fig. 2 and Fig.3, because new MLDs have been estimated with the revised method.
   -) Fig. 4, because the northern limit of the pink box used for computing the atmospheric forcing SECF has been modified.
   -) Fig. 5, we added black vertical ticks on the x-axes of plot b), which indicate times of Argo measurements.
   -) Fig. 6 and 7, because the northern limit of the pink box used for computing the preconditioning SECF has been modified.
   -) Fig. 8, because the previous point 59°N – 40°W is not centered in the SECF box, we now present the results at 58°N – 40°W, instead. Moreover, we decided to present all the anomalies in place of only anomalies larger than one-standard deviation.
   -) Fig. 10 in the previous manuscript was removed.

The new results are coherent with the results reported in the previous version of the manuscript and do not change the main conclusions of our paper.

Two of the referees indicated that the title was not adequate with the content of the paper. Consequently, we have modified the title that now reads as: Why did deep convection persist over four consecutive winters (2015-2018) Southeast of Cape Farewell?

The revised manuscript is considerably improved. We acknowledge the referees because their suggestions and comments have gratefully improved our work. All the changes can be seen in the marked-up version of the manuscript.

All the best,

Patricia ZUNINO, Herlé MERCIER and Virginie THIERRY

Interactive comment on "Two superimposed cold and fresh anomalies enhanced Irminger Sea deep convection in 2016–2018" by Patricia Zunino et al.

Femke de Jong (Referee)
femke.de.jong@nioz.nl
Received and published: 21 June 2019

Review of: "Two superimposed cold and fresh anomalies enhanced Irminger Sea deep convection in 2016-2018" by Zunino, Mercier and Thierry

The manuscript is interesting to read and a nice update on the latest convective activity in the western subpolar gyre. The separation of buoyancy fluxes into different components, including those from Ekman transport, is interesting. However it's not too surprising to see that the Ekman contribution is small given that the horizontal SST gradients are also relative small. Overall I would like to see this paper published eventually, but there is at least one major issue that need to be addressed before.

The paper hangs on the derivation of mixed layer depths and the comparison with previous years published in literature. This comparison is currently troublesome because of the substantially different way the authors derive/define the mixed layer. In fact, some of the derived mixed layers depths do not appear to be associated with actual/ recent mixed layers. Although some of the results may be robust to the methods, some others (e.g. max depth per winter, match with predicted MLDs) will clearly have to be adjusted. This should be addressed before publication.

More specifically, in a layer with turbulent mixing all properties, density, salinity and temperature, are homogenized. If the mixing occurred very recently (on the order of days ago), the homogeneous profile will still be visible all the way down to the bottom of the mixed layer. In the literature that is referred to for previous mixed layer depths (de Jong et al., 2012, 2018; de Jong in de Steur, 2016), we therefore always specified that all three properties should be mixed and of the bottoms of the mixed layer identified in each property we take the shallowest as the final mixed layer. Similar criteria were applied by group of Vage et al. in their papers. In the mooring data, as well as Argo, there are cases at the end of the winter where there remains no steplike feature visible in the density profiles at all and where a density criterion would strongly overestimate mixing, while such as steplike feature always remains visible in T and S. Therefore it is even more important to take all variables into account.

The difference between this definition of a mixed layer and that of the authors, which is a density-only criterion, is especially clear in Figure 2. The top three panels show density, salinity and potential temperature profiles from the winter of 2017. The bright blue profile, which the authors identified as having the deepest mixed layer, appears to be somewhat mixed in T and S in the upper 250 dbar (though even that is a bit questionable) but it is clearly stratified between 250 and 1400 dbar. In fact, the stratification in temperature is quite large (_0.25_C) for the Irminger Sea. The only profile in the set of four that could (potentially) qualify as having a mixed layer is the greenish profile. This would nearly half the winter maximum mixed layer depth and may also affect how well the predicted MLD match the observations.

There is code readily available to derive MLD from Argo profiles using all variables (Holte and Talley, 2009; http://mixedlayer.ucsd.edu/). I suggest the authors use this, or some adjustment of their own code, to rederive the MLD for all profiles and adjust the results of the paper accordingly.

My final main comment is that the title could be rephrased to represent the content/conclusions better. The fresh anomaly that seems to be referred to a deep one, the lowering of the halocline. The surface freshwater anomaly, which is discussed in detail elsewhere but is only touched upon here, is was not enhancing convection. It is only the cold surface anomaly that worked to enhance somewhat, but even that is only touched upon. Still, those who have not yet read the abstract may think this paper is about the big surface Sanom currently going around. While in fact, the paper focuses in detail on favorable preconditioning which is not mentioned in the title. So, it is not clear why this title was chosen.

Thank you very much for your constructive comments. In the following we answer point by point to your comments and indicate how the manuscript is going to be revised.

Following your suggestion, we revised the manuscript to define the MLDs based on density, temperature and salinity criteria (and not density criteria only). We adapted our method to include temperature and salinity criteria in addition to density criteria and we compared our results to two alternative methods of determination of the MLD previously used by de Jong et al. (2012) and Pickart et al. (2002). In our revised method, we determined the MLD as the shallowest of the three MLD estimates obtained separately from temperature, salinity and density profiles using the threshold method (de Boyer Montégut et al., 2004). The threshold criteria were the differences in property between the surface (30 m) and the MLD set to 0.01 kg m^{-3} in density (Piron et al. 2017), 0.1°C in temperature and 0.012 in salinity. The temperature threshold of 0.1°C and the salinity threshold of 0.012 were selected because they correspond to a threshold of 0.01 kg m^{-3} in density that was previously shown to perform well in the subpolar gyre (Piron et al., 2016). Indeed, MLD based on this density threshold favorably compared to those estimated by the method of Thomson and Fine (2003) as demonstrated in Piron et al. (2016; 2017) and visual inspection.
We used de Jong's methodology as follows. First we interpolated the Argo data into 10 m depth steps. Then, we estimated the standard deviations of density, temperature and salinity from the surface to each depth level. Following de Jong et al. method's, three MLD were defined as the depths were the standard deviations were smaller than 0.05 kg m^{-3}, 0.05°C and 0.005 for density, temperature and salinity, respectively. The final MLD was the shallowest of the three estimates.
The Pickart's methodology was applied as follows. We used the estimates of our threshold method as a first guess for the MLD. Then, the mean and standard deviation of the density, temperature and salinity were estimated from the surface to the initially defined MLD. Finally, we plotted the two–standard deviation envelope overlaid on the original profile. The mixed layer depth was determined as the location where the profile permanently crossed outside of the two–standard deviation envelope.
The MLDs resulting from our method are shallower than the MLD resulting from the method of de Jong et al. (see examples in figures R1 – R3). Moreover, sometimes, the MLD defined by de Jong's method in terms of temperature or salinity is not placed at the base of the mixed layer (as visually defined), e.g. profiles 6900446 – 213 (Fig. R1) or 5904772 – 33 (Fig. R3). Otherwise, the MLDs

estimated by our method are coherent with the MLDs resulting from the method of Pickart et al. (2002): see the envelopes (discontinuous vertical lines in figures R1 – R3) of mean ± two - times the standard deviation of density, salinity and potential temperature, from the surface to the MLD estimated with our method. Finally, we also compared our results with the MLDs determined using Holte & Talley (2009)'s method and available in the web. However, MLDs were not available for all our floats, e.g. float 6900446, or the method provides too shallow MLD, e.g. profile 6901171 – 101 (89 m, see Fig. R2).

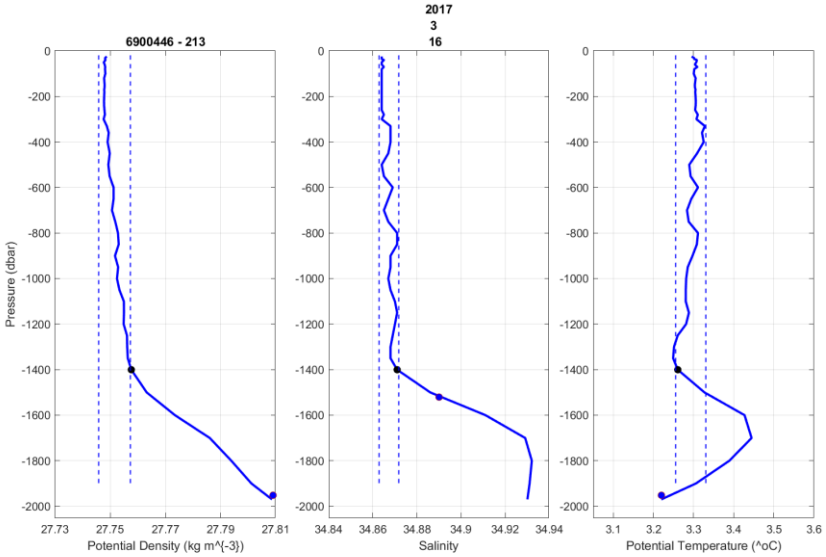

Figure R1. Vertical profiles of potential density, salinity and potential temperature of profile 6900446 - 213. The black points are the MLD estimated by our threshold method. The blue points indicate the MLDs resulting from the method of de Jong et al. (2012): in the density plot the MLD derived from density profile, in the salinity plot the MLD derived from salinity profile and in the temperature plot the MLD derived from temperature profile; the final MLD is the shallowest of the three defined MLDs. Following Pickart et al. (2002), the envelopes of mean ± two - times the standard deviation of the density, salinity and potential temperature from the surface to the MLD estimated using as a first guess for the MLD our threshold method were estimated and represented as discontinuous vertical lines.

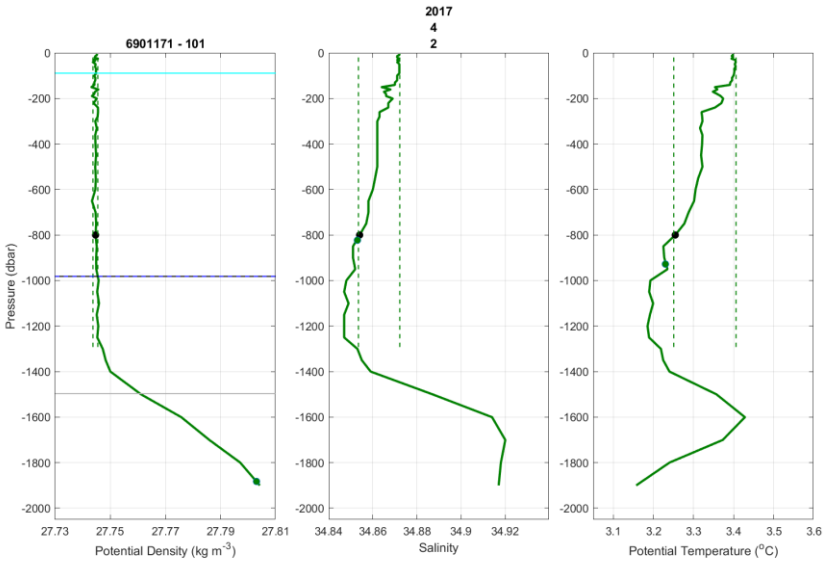

Figure R2. Same than Fig. R2 but for profile 6901171 – 101. Additionally, the horizontal lines on the left side plot represent the MLDs estimated by the Holte and Talley's method: in gray the MLD defined by the density threshold, in black the MLD defined by the density algorithm, in blue the MLD defined by the temperature threshold and in cyan the MLD defined by the temperature algorithm; note that black and blue lines are overlapping.

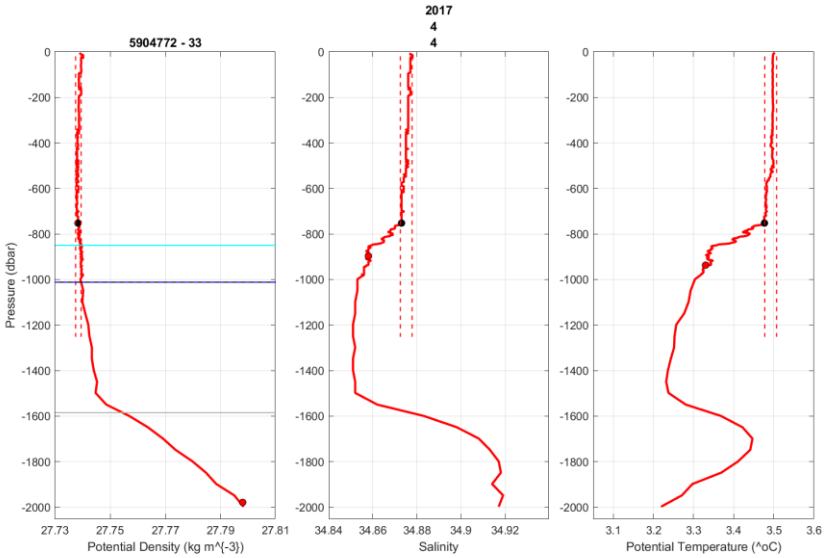

Figure R3. Same than Fig. R2 but for profile 5904772 - 33.

Because the comment of the referee focused on profiles for winter 2017, we expose in more details here the differences between the previous and the new MLD estimates for this winter 2017. First, the profile 4901809 – 35 has been eliminated because the stratification of the upper 250 m corresponds to the seasonal stratification (this profile was measured on 29th April 2017). In any case, applying the criterion of temperature threshold of 0.1°C, the MLD would be 337 m, shallower than 700 m. Second, the MLD of the profile 6901171 – 101 changes from 1250 m (the previous estimate) to 801 m (the new estimate). The MLDs estimated for profiles 6900446 – 213 and 5904772 – 33 do not change.

The MLDs of all the profiles measured Southeast Cape Farewell (SECP) during winters 2015 – 2018 were recalculated with our revised method. The positions and MLDs of the profiles showing MLDs deeper than 700 m are represented in Fig. R4. Comparing these new results with the previous results, we find that the number of profiles showing MLD deeper than 700 m decreased: 31 profiles (new) in place of 36 (previous) for winter 2015, 3 profiles (new) in place of 7 profiles (previous) for winter 2016, 3 profiles (new) in place of 4 profiles (previous) for winter 2017 and 9 profiles (new) in place of 10 profiles (previous) for winter 2018.
We have also recalculated all the properties showed in the table 1 of the previous version of the paper. Note that these properties are now estimated considering only the profiles inside the SECF box (pink box in Fig. R4.) The new results (table R1 in this document) are in line with the results of the submitted paper.

Table R1. Properties of the deep convection in the SECF (56.5°N-59.3°N, 45°W – 38°W) in winters 2015 – 2018. We show: the maximal MLD observed, the aggregate maximum depth of convection Q3, the σ_0, θ and S of the winter mixed layer formed during the convection event and n, which is the number of Argo profiles indicating deep convection. The uncertainties given with σ_0, θ and S are the standard deviation of the n values considered to estimate the mean values.

	Maximal MLD (m)	Q3 (m)	σ_0 (Kg m^{-3})	θ (°C)	S	N
W2015	1710	1205	27.733 ± 0.007	3.478 ± 0.130	34.866± 0.013	29
W2016	1575	1471	27.746± 0.002	3.388 ± 0.032	34.871± 0.003	3
W2017	1400	1251	27.745± 0.007	34.868± 0.007	3.364± 0.109	3
*W2018	*1300	*1250	*27.752± 0.004	*34.857± 0.003	*3.204± 0.069	*4
W2018	1300	1300	27.748± 0.001	34.859± 0.003	3.263± 0.031	2

*W2018 line corresponds to the properties of the mixed layer in W2018 in SEFC when the data of Float 5903102 were considered in the analysis. Finally, following the suggestion of referee 3, we decide to exclude the data of float 5903102 of our analysis because their MLDs matched with the maximal depth dived by the float.

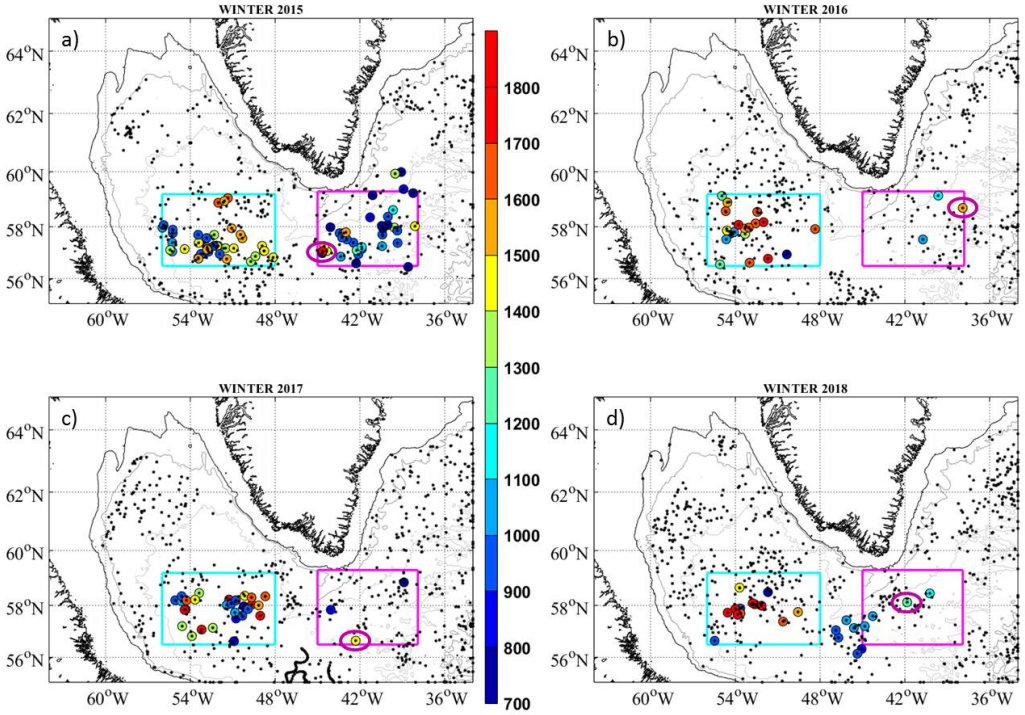

Figure R4. Positions of all Argo float north of 55°N in the Atlantic between 1 January and 30 April a) 2015, b) 2016, c) 2017 and d) 2018 (black and colored points). The colored points and color bar indicate the mixed layer depth (MLD) when MLD was deeper than 700 m. The pink circles indicate the position of the maximal MLD observed SECF each winter. The pink and cyan boxes delimit the regions used for estimating the time series of atmospheric forcing and the vertical profiles of buoyancy to be removed in the SECF region and the Labrador Sea, respectively (SECF: 56.5°N – 59.3°N and 45.0°W – 38.0°W, Labrador Sea: 56.5°N – 59.2°N and 56°W – 48°W).

We want also to clarify that in the previous version of the paper and in the new results, the deepest MLD observed in the SECF in winter 2017 was recorded by profile 6900446 – 213 and not by profile 4901809 – 35 (bright blue profile in the Fig. 2 of the previous version of the paper) as indicated by the referee. Note that for 6900446 – 213, the new MLD is the same than in the previous version of the manuscript.

Concluding, when recalculating the MLDs as suggested by the referees, the maximal MLD observed in the SECF was deeper than 1300 m in winters 2016, 2017 and 2018 (see fig. R4 and table R1). It indicates that deep convection occurred during the studied winters. This is the first important result of our paper, which does not change when recalculating the MLD.

Concerning the title, in order to avoid preconceived ideas to the reader, in the revised manuscript we change it to:
"Why did deep convection persist over four consecutive winters (2015-2018) Southeast of Cape Farewell?"

Below are some more minor comments
Introduction
Line 94. "In the Labrador Sea, deep convection occurs almost every year, yet with different intensity. In the Irminger Sea…". In the Irminger Sea some convection (_400 m) always occurs as well, and the intensity varies not unlike the Labrador Sea. Please rephrase or add a definition of "deep".
We agree. Following Piron et al. (2015), we focus on convection deeper than 700 m, which is the minimum MLD for LSW renewal. We clarified the sentence that now reads :
"In the Irminger Sea, Argo and mooring data showed that ~~deep~~ convection **deeper than 700 m** happened ~~in the Irminger Sea~~ during winters 2008, 2009, 2012, 2015 and 2016 (…)."

Data
Why is the TEOS-10 toolbox used, but profiles of theta and practical salinity are still shown instead of CT and SA?
TEOS-10 allows the computation of theta and practical salinity.

Please explain briefly why 35 is chosen as a reference.
This sentence is going to be deleted because we do not use FW in the paper. Sorry for the confusion it may have caused.

The ERA Interim reanalysis is replaced by ERA5. Best to do a check whether the results are robust to the choice of reanalysis.
It could be interesting to check the results obtained using the new ERA5 dataset. However, the first author of this paper, who processed the data, is now working in a private company and she has not the time of redoing calculations with this new database.

Method
De Boyer and Montégut criterion is not suitable for these profiles as discussed above.
See above our answer to the major comment.

The definition of the Irminger Sea, with 48_W as the limit is rather unusual. The area in Figure 1 southeast of Cape Farewell is not typically referred to as the Irminger Sea as it fall outside of the central Irminger Gyre and profiles here are very likely to have been recently advected from the Labrador Sea. To be more consistent with previous literature it would be better to split this region in three areas: the Labrador Sea, the Irminger Sea and in between the area south of Cape Farewell.
We agree that 48° W is not the limit between Labrador and Irminger Sea. When splitting the region in three areas as in Piron et al. (2017) we did not observe deep convection in the northernmost Irminger Sea (note that with the previous method of MLD computation we had a few deep MLD in the northernmost Irminger Sea in winter 2016 (those MLD corresponding to profiles not homogenous in temperature and salinity were not diagnosed with the new MLD method). In the new version of the paper we define a new pink box that we refer to as Southeast Cape Farewell (SECF) region (see Figure R4). The only change in the pink box is its northern limit: 61°N/59.3°N in the previous/revised version of the manuscript. The new box encloses all the profiles showing deep MLD during winter 2016, 2017 and 2018 Southeast of Cape Farewell. Note that the pink box is also used to estimate the atmospheric forcing and the preconditioning of the region. We recalculated it: the new results are very similar to the results shown in the previous version of the paper and do not change the conclusions of the paper.

Equation 1 and others. There are periods (.) instead of multiplication symbols. Thank you for noting it. We change all of them.

Results
What is Q3? "Q_3 is the MLD value that is exceeded by 25% of the profiles showing MLD deeper than 700 m and is equivalent to the aggregate maximum depth of convection defined by Yashayaev and Loder (2016).", as it was indicated in lines 152 – 153 of the submitted manuscript.

Part of the results paragraph will have to be rewritten when MLD are rederived.
Right, we are going to rewrite this section with the new results.

Line 268: Mean over which period?
1993 – 2016, as indicated in the figure caption of Figure 4. We add 1993 – 2016 in the text.

Line 296: This is true only when the upper 600 m already has a density close to that of the layer below (which for example could not be the case when a lot of freshwater is added). Otherwise additional buoyancy fluxes will still be required.
We are describing the buoyancy profiles from the mean (2008 – 2014) and we see that the thermal component of the buoyancy dominates the total buoyancy. We agree that if a large amount of freshwater is added to the upper ocean, we would find an important contribution of the haline component of the buoyancy, but it is not what we see in the mean (2008 – 2014) buoyancy profiles. We added Fig. 6 at the end of this sentence to make clear that we are describing the results of this figure and that the statement is not a general statement.

Section 4.4
It would be good to compare fluxes closer to the position of the observed deep MLs. These are sometimes on the very boundary of the box used to calculate the winter flux.

This comment has also motivated us to reduce the SECF or pink box. The new estimates of atmospheric forcing correspond to a reduced region closer to the position where deep convection took place.

The method used to predict the MLD does not take advection into account. This is counterintuitive because we see advection play a big role throughout winter in the field. The fact that the reanalysis do not quite match with the actual fluxes observed at OOI (Josey et al, 2018) may also be needed to take into account here. It will be interesting to see how much of a match between prediction and observation remains once new MLD are derived, likely the prediction will overestimate more.
Your comment makes sense, but note that the new estimates of MLD continue matching adequately with the predicted MLD. In the new version of the manuscript we will mention that the differences between the predicted and observed convection depth could be due to errors in the atmospheric forcing (Josey et al., 2018), lateral advection and/or spatial variation in the convection intensity within the box that was not captured by the Argo sampling.

Discussion
Line 366: This was seen throughout the 1990s and is not quite as surprising as the authors state.
We deleted "surprisingly".

Line 397: The Labrador Sea is always more favorably preconditioned, it is quite visible in the hydrographic sections and has been noted before.
The Labrador Sea is *usually* more favorably preconditioned than the Irminger Sea. However, we see that the water column from the surface to 1,300 m in winter 2017 is more favorably preconditioned in the SECF than in the Labrador Sea (see Fig. 7 in the previous version). For example, in order to homogenize the water column down to 1,300 m, 1.80 x 10^9 J m^{-2} is required in the SECF whereas 2.13 x 10^9 J m^{-2} is needed in the Labrador Sea.

Line 406: Bit of a chicken and egg problem. The halocline is also deeper in the Labrador Sea because convection is deeper there. Would rephrase.
Not really a chicken and egg problem, if you are thinking in terms of preconditioning. To clarify our point we modified the sentence as : "The deep halocline acts as a physical barrier for deep convection in both the Irminger Sea and the Labrador Sea, but because the deep halocline is deeper in the Labrador Sea than in the Irminger Sea, the preconditioning is more favorable to deeper convection in the Labrador Sea than in the Irminger Sea."

Line 416 / Fig 10. The depth is chosen such that it is always in the convective regime in the Labrador Sea, hence the nice steps. It is mostly too deep for this in the Irminger Sea, so a lot of the variability is caused by advection except in exceptionally deep convection years.
You are right and the figure is confusing even when the discussion is limited to deep convection events in the SECF region. Because of your comment and the comments of reviewer 2 we decide to delete Figure 10 and paragraph 415 - 433 in the revised manuscript.

Line 430: There is a multitude of evidence that there was very deep convection in the Irminger Sea in the 1990s (but no Argo program). The LSW was advected to the Irminger Sea in the subsequent years and hence properties converged. Please rephrase.

We decide to remove Figure 10 and paragraph 415 -433 in the revised manuscript. It does not change the conclusions of the paper.

Line 435: Bamber et al? Yes, Bamber et al. Thank you for noticing it.

Please reference papers by Dukhovsky et al (2019) and Holliday et al (2019) who both describe the fresh anomaly.
Dukhovsly et al. (2019) describe the freshwater anomaly of the 2010s, so, it does not concern the period we study in our paper.
Otherwise, we think that Holliday et al (2019) has not been published yet (V. Thierry is co-author of the paper).

Conclusions
Line 450 “in or near the Irminger Sea”
In the revised manuscript this sentence is changed to:
“During 2015 – 208 winter deep convection happened in SECF reaching deeper than 1,300 m”.

Line 473: was this only caused by advection of LSW or was the layer eroded by the 1600 m deep convection in 2016?
Our sentence was confusing. We will mention that deep convection of W2016 also favored the preconditioning for winter 2017 – 2018.

Interactive comment on "Two superimposed cold and fresh anomalies enhanced Irminger Sea deep convection in 2016–2018" by Patricia Zunino et al.

Anonymous Referee #2

Received and published: 25 June 2019

This paper reports on a very interesting analysis of recent Argo data in the subpolar North Atlantic. They claim that deep convection in the Irminger Sea, which began in 2015, persisted through 2018 because of favorable preconditioning. They perform some novel analyses and the findings will be of great interest to the community. However, I agree with the review posted by Femke de Jong, which raises issues with the way that mixed layers are defined in the study. This is central to the interpretation and conclusions of the study, and I think that at the very least some major re-framing of the work is necessary. I recommend this work for publication after major revisions.
Thank you very much for your constructive review. In the following we answer to each of your comments and describe how we are going to take into account your suggestions in the revised manuscript.

Major comments
I would like to echo de Jong's comments regarding the mixed layer depth derivation. In order to show that deep convection occurred in 2016-2018, they should show that all properties (including temperature and salinity) were homogeneous throughout, not just that a density threshold was exceeded at a very deep depth.
The three referees agreed on this point. Consequently, we have adapted our methodology to estimate the MLD considering density, temperature and salinity profiles. Please, refer to the beginning of the answer to de Jong (referee 1) in order to see how we have modified our methodology to estimate MLD. The new results (MLD and properties) do not change the main conclusions of our paper.

Regardless of the method selected by the authors in their revision they should include much more detail on it in the text as it is a central calculation. They should also be clear about how sensitive their results are to the method used and to the thresholds that are selected. They should also detail how their methods relate to the methods used by previous studies in the region.
Right, we will explain our revised methodology to estimate the MLD indicating the threshold of density, temperature and salinity used. Moreover, we will add a figure in supplementary material showing that our estimates of MLD favorable compare with the estimates resulted when using the methods of Pickart et al. (2002) or de Jong et al. (2012) as discussed at the beginning of response to referee 1.

The authors should address how sensitive their results are to the Argo float coverage, and what portion of the Argo floats present have deep mixed layers. They report how many floats have mixed layers deeper than 700m, but not how many were present. Does the percentage of floats with deep mixed layers decrease over time? The authors should comment on why they think so few Argo floats have deep mixed layers. Is it consistent with their buoyancy forcing analysis? Does the sampling in time account for some of this: i.e. Are deep mixed layers seen more commonly late in winter?
Thanks to your comment we realized that our discussion was misleading because it was based on the percentage of profiles showing deep convection during the *entire* winter, which is small by construction because only profiles at the end of winter show deep convection. We rather should have count the number of floats showing deep convection during a given year. Accordingly, we now identify the period when deep convection occurs as the period when at least one profile shows MLD > 700 m (the period begins when a profile with MLD > 700 m is detected for the first time for the given winter and it ends when there is no more profiles with MLD > 700 m). Then, we quantified the

percentage of floats with deep MLD present in that period and region (pink box in figure R4 of answer to referee 1). This information is summarized in table R2 of this document and will be included in section 4.1 of the revised manuscript. The percentage varies between 33% and 73%. In 2017, the three profiles with deep mixed layer were recorded by three different floats, all located in the southwest corner of our region. This shows that the convection area was confined to a small area of the SECF region and explains that the lowest percentage is observed in 2017.

Table R2. Sensitivity study about the Argo float coverage in the SECF region (pink box in Figure R4 of the answer to referee 1). Period is the period during which floats with deep mixed layers were observed. We indicate the total number of floats found in the SECF region during the indicated period, and the number of floats showing deep convection. Finally, the percentage of floats showing deep convection is indicated.

	Period	n floats in the region	n floats in the region with deep convection	percentage of floats in the region with deep convection
W2015	15/01/2015 to 21/04/2015	11	8	73%
W2016	22/02/2016 to 21/03/2016	4	2	50%
W2017	16/03/2017 to 04/04/2017	9	3	33%
W2018	24/02/2018 to 26/03/2018	4	2	50%

The mixed layers reported in winter 2018 are almost all to the south of Cape Farewell, and not in the Irminger Sea. Further, the TS properties in 2018 are much more similar to Labrador Sea properties than Irminger Sea properties (Figure 3). This is consistent with the SCF box properties reported in Piron et al. 2017. Some of the properties in 2016 and 2017 may also fall in that category, I don't think the author's should be calling this "Irminger Sea convection".
Right. In the revised manuscript we changed the northern limit of the pink box to 59.3°N instead of 61°N previously and refer to the pink box as Southeast Cape Farewell (SECF).

The author's show a very interesting analysis of Labrador Sea properties which are advected into Irminger Sea and contribute to the deepening of the Irminger Sea halocline (Figures 7 and 9). Is this advection limited to the 1200-1400 range they consider? How does advection from the Labrador Sea in other depth ranges fit in?
Advection from the Labrador Sea certainly contributed to vary the properties from the surface to 1000 m. However, the buoyancy budget showed that this is minor contribution compared to the buoyancy loss due to the local air-sea flux. We add a comment about it in the revised manuscript.

The title is confusing, and I wonder if, in general, the author's should shift their focus from the Irminger Sea in particular and instead focus on the important connections between the intermediate waters in the subpolar North Atlantic. I think the authors have an opportunity here to clarify that intermediate waters are formed in many places and how the connections between these basins

affect intermediate water mass properties. Their focus on salinity in addition to temperature would make this angle particularly interesting.
In the revised manuscript we change the title to: "Why did deep convection persist over four consecutive winters (2015-2018) Southeast of Cape Farewell?"
Moreover, we now mention several times the role of advection from the Labrador Sea. We also added to the discussion the following paragraph:
The Labrador Sea, SECF region and Irminger Sea are three distinct deep convection sites (e.g. Yashayaev et al., 2007; Bacon et al., 2003; Pickart et al., 2003; Piron et al., 2017). In this work, we give new insights on the connections between the different sites, showing how lateral advection of fresh LSW formed in the Labrador Sea favored the preconditioning in the SECF region fostering deeper convection."

Minor comments
The link between anthropogenic forcing and the recent convection that is drawn in the first few sentences in the abstract and throughout the introduction is a bit of a stretch. The motivation could be made more direct and convincing, and this type of speculation could remain in the discussion where it is more relevant.
Ok, in the revised manuscript we exclude the references about the anthropogenic forcing by deleting the first sentence in the Abstract and the first paragraph in the Introduction.

L109: "for the first time to our knowledge in this region" - this is a broad claim and not necessary. Ok. Deleted.

Section 3.1: Please add significant detail on the mixed layer estimation method.
Right, it has been added in the revised manuscript as indicated at the beginning of this document.

L222: The 2018 profiles with deep mixed layers are not in the Irminger Sea.
Right, as explained above, we changed the limit of the pink box and refer to our pink box as SECF.

L237: "Water masses formed are very similar" It should at least be acknowledged that they are formed much closer to the Labrador Sea than in previous years.

Right, when excluding the floats south of Cape Farewell as requested by referee 3, the properties of the water mass formed in the SECF region in W2018 is not similar to the formed in the Labrador Sea in W2018. The sentence "Water masses formed are very similar" is excluded in the new version of the manuscript.

L247: maybe instead: "heat alone" at the end of this sentence. Ok

L248: This paragraph is confusing. Perhaps referring to Figure 4 earlier on would help?
Ok, thank you for noting it. The objective of the paragraph was to show that SFek cannot be neglected in BFek. We present this point more clearly in the revision. Morevoer, in this section, we add a paragraph describing Figure 4.

L331: "despite they were also fresher" ! "despite the fact that they were also fresher"
Ok, we will change it.

L340: Refer to figure 6. Ok, we will write, "The predicted convection depths are determined as the depth at which B(zi) (Fig. 6a), equals the atmospheric forcing."

L348: Clarify what happened here. These floats only profiled down to 1,100m?

Exactly. We would rewrite the sentence as: "This result is in line with the fact that among the 10 profiles that we used to compute Q3 in W2018, 6 showed deep convection down to 1,100 m and were recorded by floats **with a maximum profiling depth** of 1,100 m, most likely leading to an underestimation of the MLD." However, this sentence is going to be deleted in the revised manuscript. In the revised paper, and following the suggestion of referee 3, we exclude from the analysis the profiles that do not extend beneath the base of the mixed layer, because it results in bias in the properties related to the mixed layer.

L351: I was also confused by the fact that the author's claim to neglect advection, but cite advection of properties from the Labrador Sea as a reason for favorable preconditioning. Perhaps remove that claim. Additionally, the fact that the T and S properties are not homogeneous goes against the idea that deep convection is occurring locally.
We agree that this paragraph was confusing. We now identify lateral advection as a possible cause for the buoyancy budget residuals. The profiles with non-homogenous TS in the mixed layers are now excluded from the analysis.

L370: hydrological ! hydrographic. Yes, hydrographic, we will change it.

L370: anomalies relative to what? Related to the mean 2002 – 2016, we added it in the text.

L383: Why would only the properties in the 1200-1400 depth range be advected? Or are they the only ones that have a profound effect? See above. Please clarify.
See answer in your comment above.

L415/Figure 10: Not sure how this figure and paragraph are linked to the rest of the study.
This figure and paragraph were not essential for the conclusions of the paper. We decide to remove them in the revised manuscript.

L470: hydrological ! hydrographic Yes, hydrographic, we will change it.

Figure 4: Note the differences between the axis ranges in the caption. This figure could be featured earlier as it provides important context.
Ok, we will write in the figure caption: "Note the differences between the axis ranges". We refer to this figure earlier in the section 4.2 of the revised manuscript.

Figure 5: From Figure 5d, it appears that the thick density layers are actually below the densities that are being ventilated in the Irminger Sea (white areas). This supports the idea that they are being advected from the Labrador Sea.
In winter 2015 and 2016 the thick density layers have a density of 32.37 Kg m^3, that corresponds to sig0 equals to 27.746 Kg m^3 which is the density of the mixed layer in the SECF (Fig. 3 in the manuscript). In winter 2017 and 2018 the thick density layers are found at denser density (32.38 Kg m^3), that corresponds to sig0 equals to 27.754 Kg m^3 which is the density of the mixed layer in the SECF for these winters (Fig. 3). These results support local formation.
Accordingly, we add at the end of the first paragraph of section 4.3: "The denser density of the core of the thick layers in 2017 -2018 compared with 2015 - 2016 agrees with the densification of the mixed layer SECF shown in Table 1 and Fig. 3."

Figure 6: Please clarify: are you using all Argo data within the box, or only the ones with deep mixed layers?
All data. To clarify, the Figure caption will be modified as, "they were calculated from **all** Argo data measured in the Irminger box (see Fig. 1) in September before the winter indicated in the legend."

Figure 7: This is a very interesting figure! Could feature more prominently and be usedto describe some key differences between the Labrador and Irminger Seas.
Right, we used this figure in the discussion (lines 394 -414) when comparing the preconditioning in the Labrador Sea and in SECF.

Reddish! red. Bluish ! blue.Ok, in the revised manuscript we change the figure caption of this figure.

Figure 8: missing a) b) c) labels on the figure. Ok, we add them.

Two superimposed cold and fresh anomalies enhanced Irminger Sea deep convection in 2016 - 2018 by Patricia Zunino, Herlé Mercier, and Virginie Thierry

Anonymous Referee #3

In this manuscript persistence of deep convection in the Irminger Sea is investigated. One winter of particularly severe atmospheric forcing and deep convection was followed by three winters of climatological strength which also had deep mixed layers. The authors quantified the buoyancy loss required for deep convection to commence each winter and concluded that the preconditioning arising from the previous winter's homogenization of the water column was a main reason for the persistence of deep convection.

I think this manuscript has the potential to be an important and valuable contribution to better understand deep water formation in the Irminger Sea /subpolar North Atlantic. However, as made clear also by the other reviewers, I have concerns about the determination of mixed-layer depths. As such, I recommend that the paper be revised before publication.

Thank you for your valuable comments; they help us improve our work. In the following we answer point by point to all of your comments and explain how we will modify the manuscript accordingly.

Major comments:

I am not convinced that automated routines, such as the threshold or split and merge methods, are particularly suitable for determining the vertical extent of the mixed layer. These routines generally perform well when applied to summer and fall profiles, when the upper ocean is stratified and there is a pronounced density difference between the mixed layer and the lower part of the profile. However, they are less accurate during periods of active convection when stratification is eroded. Furthermore, such routines cannot identify mixed layers that are isolated from the surface, either in the form of vertically stacked mixed layers or by early stages of surface restratification. Such isolated mixed layers are prevalent in the Labrador and Irminger Seas during winter (e.g. Pickart *et al.*, 2002). As pointed out by the other referees, if the density profile is considered in isolation, changes in temperature and salinity may be density-compensated such that the water column can appear to be homogenized while in reality it is not. Examples of that can be seen in Figure 2a-c (in particular 4901809 - 35). To avoid erroneous mixed-layer depths, I strongly recommend employing the semi-objective method developed by Pickart *et al.* (2002) instead of relying on automated routines.

In agreement with the three referees, we have revised our method for estimating MLD. Please see the first part of the response to de Jong (Referee 1) in order to see:

1. the specifications of our revised method for estimating MLD,
2. the comparison of MLD estimated with our revised method and estimated with other methods (de Jong et al., 2012; Pickart et al, 2002).
3. The region and profiles considered for the computation of the characteristics of the MLD (max MLD, Q3, density, temperature, salinity) formed Southeast of Cape Farewell.
4. The similarities and differences between our previous and new estimates.

Deep convection evidently took place in winter 2015 as documented by the many deep mixed layers shown in Figure 1. For winters 2016-2018, on the other hand, the vast majority of the Irminger Sea

profiles do not have particularly deep mixed layers. If widespread deep convection occurred also during these winters, there should be many more profiles with deep mixed layers. Is it possible that the mixed-layer depths determined by the automated routines are remnants of deep convection from a previous winter or from the Labrador Sea where mixed layers are generally deeper?

The percentage of profiles with deep MLD depends on the period during when we compute the statistics. Our previous method was misleading because we considered the *entire* winter for computing the statistics and not only the convection period (see also answer on this point to referee 2). We now identify the period during which deep MLDs > 700 m were observed for each winter in the Southeast Cape Farewell (SECF) region (pink box in Fig. R4 in referee 1 answer) (see answer to reviewer 2 for more details). Then, we quantified the percentage of floats that measured deep MLD in the region and during the period of deep convection. The results are shown in table R2. The lower % is found for winter 2017, but it is still substantial and reflects the fact by the fact that the floats showing deep MLD were found southwest of the SECF box suggesting that convection did not occur over the full box. The results of this sensitive study will be added to the section 4.1 of the revised manuscript.

Table R2. Sensitivity study about the Argo float coverage in the SECF region (pink box in Figure R4 in the answer to referee 1). Period is the period during which floats with deep mixed layers were observed. We indicate the total number of floats found in the SECF region during the indicated period, and the number of floats showing deep convection. Finally, the percentage of floats showing deep convection is indicated.

	Deep convection period	n floats in the region	n floats in the region with deep convection	% of floats in the region with deep convection
W2015	15/01/2015 to 21/04/2015	11	8	73%
W2016	22/02/2016 to 21/03/2016	4	2	50%
W2017	16/03/2017 to 04/04/2017	9	3	33%
W2018	24/02/2018 to 26/03/2018	4	2	50%

We do not think that the observed MLD are remnants of deep convection from a previous winter or from the Labrador Sea because the new estimates of MLD are from profiles homogenous in terms of density, temperature and salinity. Most importantly, the fact that the 1D-buoyancy budget is nearly closed (section 4.3) is also an indication that deep convection occurred locally in the SECF box during winters 2016, 2017 and 2018.

To get a more robust estimate of convection in the subpolar North Atlantic these winters, I suggest dispensing with the 700 m “deep convection” criterion and showing if not every mixed layer at least the 50-80% deepest mixed layers encountered by each float every winter. That would remove shallow mixed layers arising from early phases of the seasonal evolution of the mixed layer and profiles obtained within stratified eddies, while the remaining mixed layers would allow for more robust quantification of the general depth of convection.

OK, this seems to be a nice idea, but it would bias low the estimate of convection depth if the statistics of MLD were made using the profiles for the entire winter. The criteria should be applied to the convection period that we select here by considering profiles deeper than 700 m because it is the minimum depth that should be reached for LSW renewal. If apply to those profiles your criteria would not be much different from our Q3. Note that our estimate of convection depth based on the statistical criteria Q3 is equivalent to the aggregate maximal convection depth used by Yashayaev and Loder (2017) and allows direct comparison with this author's results.

Profiles that do not extend beneath the base of the mixed layer (there may be some examples in Figure 2d-f) would result in a shallow bias of the mixed-layer depth estimate and should be excluded from the analysis.
We agree. These profiles located between 48°W and 45°W are not consider in our new results.

Specific comments:
Line 95:
It should be: "...Argo and mooring data..." Corrected

Lines 106 and 361:
Mixed layers exceeding 1400 m depth were determined also from shipboard measurements in the Irminger Sea in April 2015 (Fröb *et al.*, 2016). We add this reference to the revised manuscript.

Line 122:
If the TEOS-10 convention is used, conservative temperature and absolute salinity should be used instead of potential temperature and salinity.
TEOS-10 allows the computation of theta and practical salinity.

Line 123:
Please explain why a salinity of 35 was chosen as a reference value.
This sentence is deleted in the manuscript because we do not use FW in the paper. Sorry for the confusion it may have caused.

Line 124:
Please provide more information about the gridded products. Are different time periods and resolutions the only difference between the products? What are the errors, in particular for the EN4 product which extends back to 1900 and covers some very data-sparse periods?
ISAS and EN4 are optimal interpolation of in situ data, but the optimal interpolation method is not exactly the same in both products due to different choices for the spatial and temporal correlation functions used for the optimal interpolation. Details about both databases are described in the references given in the manuscript (Gaillard et al., 2016; Kolodziejczyk et al., 2017; Good et al. 2013). Note that we used EN4 data from 1993 afterwards and that the monthly temperature and salinity fields at a given time only depends on the data found in a short time window around the date of the analysis. The data sparse-period at the beginning of the 1900 did not influence our results.

Line 130:

Does the net air-sea heat flux include radiative fluxes or only turbulent fluxes?
It includes both radiative and turbulent fluxes. We indicate it in the revised manuscript.

Line 149:
I do not think that 48◦W is commonly used as a border between the Labrador and the Irminger Seas. Many of the deep mixed layers were recorded directly south of Greenland, in a region that is not really part of either the Labrador or the Irminger Seas.
Ok, the limit at 48°W was used just to include in the analysis of the MLD properties the profiles found between 48°W and 45°W in 2018. In the revised computation we used only profiles inside the pink box which limit is at 45°W and we now refer to the pink box as Southeast Cape Farewell (SECF) instead of Irminger Sea. Note that the northern limit of the box is changed from 61°N to 59.3°N. We calculated the atmospheric forcing and the preconditioning considering this new box limit and it does not change the main results and conclusions of our work.

Line 156 and elsewhere:
Please insure that all papers cited in the text are included in the References section. For example is Gill (1982) missing. Ok, thank you for noting it.

Line 174:
How was the depth of the Ekman layer estimated?

We used the Ekman transport and we considered that the SST is representative of the temperature in the Ekman layer. We will clarify this point in the revision.

Line 179:
For consistency, it might be better to use SST also from the EN4 product.
Ok, we have estimated the Ekman Buoyancy Flux (BFek) using EN4 SST.
The horizontal Ekman Buoyancy flux in the SECF region (pink box in Fig. R4 in response to referee 1), accumulated from 1 September to 31 August the year after was estimated with: i) with EN4 SST and EN4 SSS and ii) with ERA SST and EN4 SSS; they are represented in Figure R5. Both time series show the same behavior but the results obtained with EN4 SSS and EN4 SST are smoother than the results obtained with ERA SST and EN4 SSS. Thank you for your comment, we switched to EN4 SST.

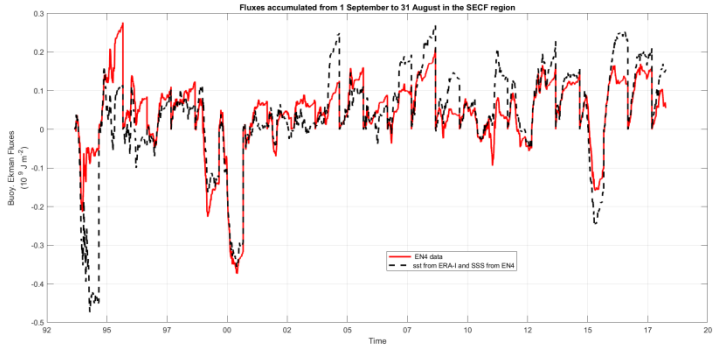

Figure R5. Horizontal Ekman Buoyancy flux in the SECF region (56.5° - 59.3°N, 45°W – 38°W), accumulated from 1 September to 31 August the year after estimated: i) with EN4 SSS and EN4SST and ii) with ERA SST and EN4 SSS.

Line 185:
It should be: "...most of the Argo profiles..." Corrected.

Line 197:
It should be: "...to be removed (B(zi)) from the late summer density profile..." Corrected.

Line 234:
Salted, in this context, is not appropriate. "Became saltier" would be a better expression. Corrected.

Line 284:
If B remained nearly constant, does that imply that restratification and advection are unimportant?

It means that the homogeneous layer (600 – 1400 m) formed at the end of winter was not destroyed by the advection by eddies and large scale circulation during the following spring and summer.

Line 297:
Units (m) are missing after 800-1000. Corrected.

Line 321:
What was the basis for choosing the point 59◦N, 40◦W?
Our objective here was to see the evolution of the anomalies in depth and in time. Therefore we choose a point, 59°N, 40°W, in the middle of the box. The result is not sensitive to the location of the point inside the pink box. This information is added to the revised manuscript. In the revised manuscript we present the same figure at 58°N, 40°W, which is centered in the new pink box, instead that at 59°N, 40°W.

Line 377:
If convection exceeded 1400 m in winter 2014-15 (e.g. Fröb *et al.*, 2016), why is it unlikely that this layer was locally formed?
Right, we cannot exclude that the convection of winter 2014-15 cause salinity decrease in the water column. We slightly modified this paragraph in the revised manuscript.

Line 382: The papers by Lavender *et al.* (2000) and Straneo *et al.* (2003) could also be cited here. Ok, we add them to the revised paper.

Line 383: Corroborated is misspelled. Right.

Line 388:
If deep convection occurs every year, perhaps the definition of deep convection should be revised.
This sentence is confusing. In the revised manuscript, this sentence is written as:
"We now compare the atmospheric forcing and the preconditioning of the water column in the SECF region with those of the nearby Labrador Sea where deep convection happens almost every year."

Line 403:
It should be: "...the deep halocline was successively deepening..." Right, thank you.

Line 410:
I am sceptical of the claim that the deepest convection-depth ever observed in the Labrador Sea occurred in winters 2016-2018. Very likely convection in the successive high-NAO winters of the early l990s substantially exceeded convection in winters 2016-2018. At that time mixed-layer depths were at least 2300 m (e.g. Avsic *et al.*, 2006).
Yes, you are right. So, we add to the sentence "since the beginning of the Argo period".

Lines 419 and 421:
Density units are not capitalized consistently. Ok.

Line 425:
It should be: "...observed in both basins..." Right, thank you.

Line 430:
There were no wintertime measurements in the Irminger Sea in the early 1990s, but there is strong indirect evidence that deep convection occurred in the Irminger Sea at that time (see for example publications from the group of R. Pickart).
Right, there are evidences that deep convection occurred in the Irminger Sea in early 1990s (Pickart et al., 2003).
In any case, the three referees find something wrong in this paragraph and Figure 10. Because this paragraph and figure is not important for the conclusions of our paper we decide to remove them in the revised version of the paper.

Line 481:
Acknowledgement is misspelled. Right, thank you.

Lines 519 and 522:
The name de Jong is inconsistently capitalized. Right, corrected.

Figure 5:
Please indicate, for example using tick marks along the top axis, when Argo float profiles were available in the Irminger Sea.
Ok, we add the tick marks in plot 5b.

~~Two superimposed cold and fresh anomalies enhanced Irminger Sea deep convection in 2016 – 2018~~

Why did deep convection persist over four consecutive winters (2015-2018) Southeast of Cape Farewell?

Patricia ZUNINO[1], Herlé MERCIER[2] and Virginie THIERRY[3].

1 Altran Technologies, Technopôle Brest Iroise, Site du Vernis , 300 rue Pierre Rivoalon, 29200 Brest, France

2 CNRS, University of Brest, IRD, Ifremer, Laboratoire d'Océanographie Physique et Spatiale (LOPS), IUEM, ZI de la pointe du diable, CS 10070 - 29280 Plouzané, France

3 Ifremer, University of Brest, CNRS, IRD, Laboratoire d'Océanographie Physique et Spatiale (LOPS), IUEM, ZI de la pointe du diable, CS 10070 - 29280 Plouzané, France

Corresponding author: patricia.zuninorodriguez@altran.fr

ABSTRACT

~~While Earth system models project a reduction, or even a shut-down, of deep convection in the North Atlantic Ocean in response to anthropogenic forcing~~ After more than a decade of shallow convection, deep convection returned to the Irminger Sea in 2008 and occurred several times since then to reach exceptional depths > 1,500 m in 2015 and 2016. Additionally, deep mixed layers larger than 1600 m were also reported Southeast of Cape Farewell in 2015. In this context, we used Argo data to show that deep convection occurred Southeast of Cape Farewell (SECF) in 2016 and persisted ~~in the Irminger Sea~~ during two additional years in 2017 and 2018 with maximum convection depth ~~>~~larger than 1,300 m. In this article, we investigate the respective roles of air-sea buoyancy flux and preconditioning of the water column (ocean interior buoyancy content) to explain this exceptional 4-year persistence of deep convection SECF. We analyzed the respective contributions of the heat and freshwater components.~~; we quantified them in terms of buoyancy and analyzed both the heat and freshwater components~~. Contrary to the very negative air-sea buoyancy flux that was observed during winter 2015, the buoyancy fluxes over the ~~Irminger Sea~~SECF region during winters 2016, 2017 and 2018 were close to climatological average. We estimated the preconditioning of the water column as the buoyancy that needs to be removed (B) from the end of summer water column to homogenize the water column down to a given depth. B was lower for winters 2016 – 2018 than for the mean 2008 – 2015 winter mean, due especially to ~~, including~~ a vanishing stratification from 600 m down to ~1,300 m. It means that less air-sea buoyancy loss was necessary to reach a given convection depth than in the mean and once convection reached 600 m little additional buoyancy loss was needed to homogenize the water column down to 1,300 m. We showed that the decrease in B was due to the combined effects of the local~~a~~ cooling of the intermediate water (200 – 800 m) and the advection of a negative S anomaly~~a decrease in salinity~~ in the 1,200 – 1,400 m layer. This favorable preconditioning permitted the very deep convection observed in 2016 – 2018 despite the atmospheric forcing was close to the climatological average.

1. INTRODUCTION

~~The physical and biogeochemical properties of the oceans are experiencing unprecedented changes as a result of the human activities (IPCC, 2013). For this reason, a challenge for the oceanographic community is to disentangle the natural and anthropogenic components of the ocean variability. Under Climate Change scenarios, Earth system models predict a warmer climate, an increase in freshwater flux into the ocean due to ice melting (Bamber et al., 2018)), a slow down of the Meridional Overturning Circulation (Rahmstorf et al., 2015), and a reduction or shut-down of deep convection in the North Atlantic (Brodeau & Koenigk, 2016). In this paper, we study the recent evolution of deep convection in the northern North Atlantic.~~

Deep convection is the result of a process by which surface waters loose buoyancy due to atmospheric forcing and sink into the interior ocean. It occurs only where specific conditions are met including large air-sea buoyancy loss and favorable preconditioning (i.e. low stratification of the water column) (Marshall & Schott, 1999). In the Subpolar North Atlantic (SPNA), deep convection takes place in the Labrador Sea, South of Cape Farewell and in the Irminger Sea (Kieke & Yashayaev, 2015; Pickart et al. 2003; Piron et al. 2017). Deep convection connect~~s~~ing the upper and lower limbs of the Meridional Overturning Circulation (MOC) and transferring climate change signals from the surface to the ocean interior.

~~The observation and description of~~ Observing deep convection is difficult because ~~deep convection~~it happens on short time and small spatial scales and during periods of severe weather conditions ~~at very short space and time scales~~ (Marshall & Schott, 1999) ~~and during periods of severe weather conditions~~. The onset of the Argo program (http://www.argo.net/) at the beginning of the 2000s, has considerably increased the number of available~~availability of~~ oceanographic data throughout the year. Although the sampling characteristics of Argo are not adequate to observe the smaller scales associated with the process itself, ~~this dataset~~Argo data allow~~ed~~ the description of the overall intensity of the event, and the characterization of the properties of the water masses formed in the winter mixed layer as well (e.g., Yashayaev and Loder, 2017). ~~The challenge now is to evaluate how deep convection could evolve under climate change.~~

In the Labrador Sea, deep convection occurs ~~almost~~ every year, yet with different intensity (e.g., Yashayaev and Clarke, 2008; Kieke and Yashayaev, 2015). In the Irminger Sea, Argo and mooring~~s~~ data showed that deep convection deeper than 700 m happened ~~in the Irminger Sea~~ during winters 2008, 2009, 2012, 2015 and 2016 (Väge et al., 2009; de Jong et al., 2012; Piron et al. 2015; de Jong & de Steur, 2016; Fröb et al., 2016; Piron et al. 2017 ; de Jong et al., 2018). Moreover, in winter 2015,

deep convection was also observed south of Cape Farewell (Piron et al., 2017). Excluding the winter 2009 when the event was possible thanks to a favorable preconditioning set the winter before (de Jong et al. 2012), all events coincided with strong atmospheric-forcing (air-sea heat loss). Prior to 2008, only few deep convection events were reported because the mechanisms leading to it were not favorable (Centurioni and Gould, 2004) or~~and~~ because the observing system was not adequate (Bacon, 1997; Pickart et al., 2003). Nevertheless, the hydrographic properties from the 1990s suggested that deep convection reached as deep as 1,500 m in the Irminger Sea during winters 1994 and 1995 (Pickart et al., 2003), and as deep as 1,000 m south of Cape Farewell during winter 1997 (Bacon et al., 2003).

The convection depths that were reached in the Irminger Sea and south of Cape Farewell at the end of winter 2015 ~~was~~ were the deepest observed in ~~the Irminger Sea~~these regions since the beginning of the 21st century (de Jong et al., 2016; Fröb et al., 2016; Piron et al., 2016). In this work, we show that deep convection also happened in a region between south of Cape Farewell and the Irminger Sea (the pink box in Figure 1) every~~each~~ winter ~~in the Irminger Sea during the period~~from 2016 ~~–~~to 2018. We investigate the respective role of atmospheric forcing (air-sea buoyancy flux) and preconditioning (ocean interior buoyancy content) in setting the convection intensity. We ~~evaluate them in terms of air-sea buoyancy flux and buoyancy content and, for the first time to our knowledge in this region, we~~also disentagle the relative contribution of salinity and temperature anomalies to the preconditioning. The paper is organized as follow. The data are described in Sect. 2. The methodology is explained in Sect. 3. We expose our results in Sect. 4 and discuss them in Sect. 5. Conclusions are listed in Sect. 6.

2. DATA

We used temperature (T), salinity (S) and pressure (P) data measured by Argo floats north of 55°N in the Atlantic Ocean. These data were collected by the International Argo program (http://www.argo.ucsd.edu/, http://www.jcommops.org/) and downloaded from the Coriolis Data Center (http://www.coriolis.eu.org/). Only data flagged as good (quality Control < 3, Argo Data Management Team, 2017) were considered in our analysis. Potential temperature (θ), density (ρ) and potential density anomaly referenced to the surface and 1000 dbar (σ_0 and σ_1, respectively) were estimated from T, S and P data using TEOS-10 (http://www.teos-10.org/). ~~As in Zunino et al. (2017), we define freshwater as: $FW = \frac{35-S}{35}$.~~

We used two different gridded products of ocean T and S: EN4 and ISAS. ISAS (Gaillard et al., 2016; Kolodziejczyk et al., 2017) is produced by optimal interpolation of *in situ* data. It provides monthly fields, at 152 depth levels, at 0.5° resolution, from 2002 to 2015. Near real time data are also availaible for 2016 and 2018. EN4 (Good et al., 2013) is an optimal interpolation of *in situ* data; it provides monthly T and S at 1° spatial resolution and at 42 depth levels, for the period 1900 to present.

Net air-sea heat flux (Q, the sum of radiative and turbulent fluxes), evaporation (E), precipitation (P), wind stress (τ_x and τ_y) and sea surface temperature (SST) data were obtained from ERA-Interim reanalysis (Dee et al., 2011). ERA-Interim provides data with a time resolution of 12h and a spatial resolution of 0.75°, respectively. The air-sea freshwater flux (FWF) was estimated as E - P.

We used monthly Absolute Dynamic Topographic (ADT), which was computed from the daily 0.25° -resolution ADT data provided by CMEMS (Copernicus Marine and Environment Monitoring Service, http://www.marine.copernicus.eu).

3. METHODS

3.1 Quantification of the deep convection

~~In order to characterize the convection in the Irminger Sea and Labrador Sea in winters 2015-2018, we estimated the mixed layer depths (MLD) for all Argo profiles collected in the SPNA north of 55°N from 1st January to 30th April of each year (Fig. 1). Following Piron et al. (2016), the MLD was estimated by the threshold method (de Boyer Montégut et al., 2004) and the split and merge method (Thomson and Fine, 2003) complemented by visual inspection of the vertical profiles of ρ when the two estimates differed.~~

We characterized the convection in the SPNA in winters 2015-2018 by estimating the mixed layer depths (MLD) for all Argo profiles collected in the SPNA north of 55°N from 1st January to 30th April of each year (Fig. 1). The MLD was estimated as the shallowest of the three MLD estimates obtained by applying the threshold method (de Boyer Montégut et al., 2004) to θ, S and ρ profiles separately. The threshold method computes the MLD as the depth at which the difference between the surface (30 m) and deeper levels in a given property is equal to a given threshold. In case visual inspection of the winter profiles showed a thin stratified layer at the surface, a slightly deeper level (<150 m) was considered as surface reference level. Following Piron et al. (2017), this threshold was taken equal to 0.01 kg m^{-3} for ρ. For θ and S, we selected thresholds of 0.1°C and 0.012 respectively because they

correspond to the threshold of 0.01 kg m^{-3} in ρ. The latter was previously shown to perform well in the subpolar gyre on density profiles (Piron et al., 2016). Our MLD estimates are comparable to those obtained using MLD determination based on Pickart et al. (2002)'s and de Jong et al. (2012)'s methods (see section S1, Fig. S1 and Fig. S2 in supplementary material).

In this paper, deep convection is characterized by profiles with MLD deeper than 700m (colored big points in Fig. 1) because it is the minimum depth that should be reached for Labrador Sea Water (LSW) renewal (Yashayaev et al., 2007; Piron et al. 2016).

The winter MLD and the associated θ, S and ρ properties were examined for the Labrador Sea and the SECF region by considering the profiles inside the cyan and pink boxes in Fig. 1, respectively. Those two boxes were defined to include all Argo profiles with MLD deeper than 700 m during 2016 – 2018 and the minimum of the monthly ADT for either the SECF region or the Labrador Sea. No deep MLD was recorded in the northernmost part of the Irminger Sea during this period. ~~the Irminger Sea, separately. We used 48°W as the limit between the Irminger Sea and the Labrador Sea.~~ We computed the maximum MLD and the MLD third quartile (Q_3) from profiles with~~(we only used~~ MLD greater than 700m in each of the two boxes separately ~~for the computation of Q_3)~~. Q_3 is the MLD value that is exceeded by 25% of the profiles and is equivalent to the aggregate maximum depth of convection defined by Yashayaev and Loder (2016). The properties (ρ, θ and S) of the mixed layers ~~formed each winter~~ were defined for each winter as the vertical mean from 200 m to the MLD of all ~~the n~~ profiles with MLD deeper than 700 m. For further use, we define the deep convection period as follows. For a given winter, the deep convection period begins the day when the first profile with a deep (>700m) mixed layer is detected and ends the day of the last detection of a deep mixed layer.

3.2. Time series of atmospheric forcing

The air-sea buoyancy flux (B_{surf}) was calculated as the sum of the contributions of Q and FWF (Gill, 1982; Billheimer & Talley, 2013). It reads:

~~$$B_{surf} = \frac{\alpha . g}{\rho_0 . c_p} . Q - \beta . g . SSS . FWF$$~~

$$B_{surf} = \frac{\alpha\, g}{\rho_0\, c_p}\, Q - \beta\, g\, SSS\, FWF \qquad \text{Eq. (1)}$$

Where α and β are the coefficients of thermal and saline expansions, respectively, estimated from surface T and S. The gravitational acceleration g is equal to 9.8 m s^{-2}, the reference density of sea

water ρ_0 is equal to 1026 kg m^{-3} and heat capacity of sea water C_p is equal to 3990 J kg^{-1} $°C^{-1}$. SSS is the sea surface salinity. Q and FWF are in W m^{-2} and m s^{-1}, respectively.

For easy comparison with previous results that only considered the heat component of the total air-sea flux (e.g. Yashayaev & Loder, 2017; Piron et al., 2017; Rhein et al., 2017), B_{surf}, in m^2 s^{-3}, was converted to W m^{-2} following Eq. (2) and noted B^*_{surf}

~~$B^*_{surf} = \frac{\rho_0 . c_p}{g . \alpha} . B_{surf}$~~

$$B^*_{surf} = \frac{\rho_0 \, c_p}{g \, \alpha} \, B_{surf} \qquad \text{Eq. (2)}$$

The FWF was also converted to W m^{-2} using:

~~FWF*= FWF . β . SSS. $\frac{\rho_0 . c_p}{\alpha}$~~

$$\text{FWF*= FWF } \beta \; SSS \; \frac{\rho_0 \, c_p}{\alpha} \qquad \text{Eq. (3)}$$

We also computed the horizontal Ekman buoyancy flux (BF_{ek}), ~~and their components~~which can be decomposed into the horizontal Ekman heat flux (HF_{ek}) and the horizontal Ekman salt flux (SF_{ek})~~, for which $BF_{ek} = SF_{ek} - HF_{ek}$~~. Noting:

~~$BF_{ek} = -g . (U_e \partial_x SSD + V_e \partial_y SSD) . \frac{C_p}{\alpha . g}$ Eq. (4)~~

~~$HF_{ek} = -(U_e \partial_x SST + V_e \partial_y SST) . \rho_0 . C_p$ Eq. (5)~~

~~$SF_{ek} = -(U_e \partial_x SSS + V_e \partial_y SSS) . \frac{\beta . \rho_0 . C_p}{\alpha .}$ Eq. (6)~~

$$BF_{ek} = -g \; (U_e \partial_x SSD + V_e \partial_y SSD) \frac{C_p}{\alpha . g} \qquad \text{Eq. (4)}$$

$$HF_{ek} = -(U_e \partial_x SST + V_e \partial_y SST) \; \rho_0 \; C_p \qquad \text{Eq. (5)}$$

$$SF_{ek} = -(U_e \partial_x SSS + V_e \partial_y SSS) \; \frac{\beta \; \rho_0 \; C_p}{\alpha} \qquad \text{Eq. (6)}$$

$BF_{ek} = SF_{ek} - HF_{ek}$.~~where~~ U_e and V_e are the eastward and westward components of the Ekman horizontal transport estimated from the wind stress meridional and zonal components. SSD, SST and SSS are ρ, T and S at the surface of the ocean. BF_{ek}, HF_{ek} and SF_e are in J s^{-1} m^{-2}. Because ERA-Interim does not supply SSD or SSS, the monthly S at 5 m depth from EN4 were interpolated on the same time and space grid as the air-sea fluxes from ERA-Interim (12h and 0.75°, respectively). SSD was

estimated from those interpolated EN4 data (SST and SSS). Properties at 5 m depth were considered to be representative of the Ekman layer. ~~SST of ERA-Interim and interpolated S of EN4~~. Data at locations where the ocean bottom was~~points~~ shallower than 1000 m were excluded from the analysis to avoid regions covered by sea-ice.

Following Piron et al. (2016), the time series of atmospheric forcing were estimated for the ~~Irminger Sea~~SECF region and the Labrador Sea as follows. First, the gridded air-sea flux data and the horizontal Ekman fluxes were averaged over the pink (SECF region) and cyan (Labrador Sea) boxes (Fig. 1)~~the region, pink and cyan boxes in Fig. 1 for the Irminger Sea and Labrador Sea, respectively. The boxes, which are representative of the convection regions, were defined to include most of Argo profiles with MLD deeper than 700 m and the minimum of the monthly ADT for either the Irminger Sea or the Labrador Sea~~. Second, we estimated the accumulated fluxes from 1 September to 31 August the year after. Finally, we computed the time series of the anomalies of the accumulated fluxes from 1 September to 31 August with respect to the 1993 – 2016 mean.

Finally, in order to quantify the net intensity of the atmospheric forcing over the winter, we computed estimates of ~~air-sea~~ B_{surf}* + BF_{ek} fluxes accumulated from 1 September to 31 March the year after. Following Piron et al. (2017), ~~T~~the associated errors were calculated by a Monte Carlo simulation using 50 random perturbations ~~as the standard deviation of 50 estimates~~ of Q, FWF and B_{surf} ~~perturbed by one standard deviation of their spatial mean~~. The error amounted to 0.05 J m^2 , 0.04 and 0.03 J m^{-2} for B_{surf}*, Q and FWF*, respectively. The error of the horizontal Ekman transport was also estimated by a Monte Carlo simulation and amounted to 0.04 J m^{-2}.

3.3. Preconditioning of the water column

The preconditioning of the water column was evaluated in terms of buoyancy that has to be removed ($B(zi)$) to the late summer density profile to homogenize it down to a depth *zi*. It reads:

~~$B(zi) = \frac{g}{\rho_0} * \sigma_0(zi) * zi - \frac{g}{\rho_0}\int_{z_i}^{o} \sigma_0(z)dz$~~

$$B(zi) = \frac{g}{\rho_0}\ \sigma_0(zi)zi\ -\ \frac{g}{\rho_0}\int_{z_i}^{o}\sigma_0\ (z)dz \quad \text{Eq. (7)}$$

σ_0(z) is the vertical profile of potential density anomaly estimated from the profiles of T and S measured by Argo floats in September in the given region (pink or cyan box in Fig. 1).

Following Schmidt and Send (2007), we split B into a temperature (B_θ) and salinity (B_S) term as:

~~$B_\theta(zi) = -(g * \alpha * \theta(zi) * zi - g * \alpha * \int_{zi}^{o}\theta(z)\,dz)$ Eq. (8)~~

~~$B_S(zi) = g * \beta * S(zi) * zi - g * \beta * \int_{zi}^{o} S(z)dz$~~ ~~Eq. (9)~~

$B_\theta(zi) = -(g\ \alpha\ \theta(zi)\ zi - g\ \alpha \int_{zi}^{o} \theta(z)\ dz)$ Eq. (8)

$B_S(zi) = g\ \beta\ S(zi)\ zi - g\ \beta \int_{zi}^{o} S(z)dz$ Eq. (9)

In order to compare the preconditioning~~B~~ with the heat to be removed and/or air-sea heat fluxes, B, B_θ and B_S are reported in ~~the buoyancy results in m^2 s^{-2} were converted to~~ J m^{-2}.

B, B_θ and B_S were estimated for a given year from the mean of all September profiles of B, B_θ and B_S. The associated errors were estimated as std(B)/√n, where n is the number of profiles used to compute the September mean values.

4. RESULTS

4.1. Intensity of deep convection and properties of newly formed LSW

We examine the time-evolution of the ~~Irminger Sea~~ winter mixed layer SECF since the exceptional convection event of winter 2015 (W2015 hereinafter) (Table 1 and Fig. 3). In W2015 we recorded a maximum MLD of ~~1,715~~1,710 m south of Cape Farewell (Fig. 1a), in line with Piron et al. (2017). The maximum MLD of 1,575 m observed for W2016 (Fig. 1b) is compatible with the MLD > 1,500 m observed in a mooring array in the central Irminger Sea by de Jong et al. (2018). For W2015 and W2016, Q3 was 1,205 m and 1,471 m, respectively (Table 1). ~~We additionally showed that for both winters Q3 was about 1300 m (Table 1). Now, we describe the convection of W2017 and W2018.~~ In W2017, deep convection was defined from ~~four~~ three Argo profiles ~~in the Irminger Sea~~ (see Fig. 1c and Fig. 2a-c). The maximum MLD of 1,400 m was observed on 16th March 2017 at 56.65°N – 42.30°W. ~~The aggregate maximum depth of convection Q3 coincided with the maximum MLD because the estimates are based on only four profiles.~~ In W2018, ~~ten profiles showed MLD deeper than 700 m in the Irminger Sea (Fig. 1d, 2d-f). T~~the maximum MLD of 1,300 m was observed on 24 February at 58.12°N, 41.84°W. (Fig. 1d, 2d-f). Float 5903102 measured MLD of 1,100 m South of Cape Farewell (Fig. 1d), but the estimated MLDs coincided with the deepest levels of measurement of the float so that these estimates, possibly biased low (see Fig. 2d-f), were discarded from our analysis. ~~The aggregate maximum depth of convection Q3 was 1,100 m. Float 5903102, which was localized South of Cape Farewell, did not profile deeper than 1,100 m in any of its six cycles (see Fig. 2d-f); it is therefore possible that the MLD was deeper than 1,100 m in these profiles. Excluding the data of Float 5903102, the aggregate maximum depth of convection Q3 is 1,300 m.~~ These results reveal that convection deeper than 1,300 m occurred during four consecutive winters in the Irminger Sea.

Although the number of floats showing deep convection in W2017 and W2018 was small (3 and 2 floats), it represented a significant percentage of the floats operating in the SECF box at that time. The percentage of floats showing deep convection in the SECF region was computed for the deep convection periods defined from 15 January 2015 to 21 April 2015, 22 February 2016 to 21 March 2016, 16 March 2017 to 4 April 2017 and 24 February 2018 to 26 March 2018. The longest period of deep convection occurred in W2015, the shortest in 2017. The percentage of floats showing deep convection during the deep convection period are 73%, 50%, 33 % and 50%, for winters 2015, 2016, 2017 and 2018, respectively. The lowest % is found for W2017, but it is still substantial. It might reflect that for this specific year floats showing deep MLD were found in the southwestern corner of the SECF box only, suggesting that convection did not occur over the full box.

The properties (σ_0, S and θ) of the end of winter mixed layer were estimated for the four winters (Table 1 and Fig. 3). We observed that, between W2015 and W2018, the water mass formed by deep convection significantly densified and cooled by 0.019 kg m^{-3} and ~~0.306~~0.215°C, respectively (see Table 1).

In the Labrador Sea, Q3 increased from 2015 to 2018 (see Table 1). Deep convection observed in the Labrador Sea in W2018 was the most intense since the beginning of the Argo era (see Fig. 2c in Yashayaev & Loder, 2016). From W2015 to W2018, newly formed LSW cooled, salted and densified by 0.134°C, 0.013 and 0.023 kg m^{-3}, respectively (Table 1).

The water mass formed ~~in the Irminger Sea~~SECF is warmer and saltier than that formed in the Labrador Sea (Fig. 3)~~; the exception is in W2018 when the characteristics of the water masses formed in each of the basins are very similar~~. The deep convection in ~~the Irminger Sea~~SECF is always shallower than in the Labrador Sea. Both results are discussed later in Sect. 5.

4.2. Analysis of the atmospheric forcing ~~in the Irminger Sea~~Southeast of Cape Farewell

The seasonal cycles of B_{surf}* and Q are in phase and of the same order of magnitude, while ~~the~~ FWF* , which is positive and one order of magnitude lower than Q ~~and~~ , does not present a seasonal cycle (Fig. ~~S1~~S3). The means (1993 – 2018) of the cumulative sums from 1 September to 31 March of Q, FWF* and B_{surf}* estimated over the ~~Irminger~~ SECF box (Fig. 1) are - 2.46 ± 0.43 x 10^9 J m^{-2}, 0.28 ± 0.10 x 10^9 J m^{-2} and - 2.22 ± 0.49 x 10^9 J m^{-2} ~~- 2.52 ± 0.43 x 10^9 J m^{-2}, 0.31 ± 0.11 x 10^9 J m^{-2} and - 2.26 ± 0.51 x 10^9~~ J m^{-2}, respectively. Despite B_{surf}* is mainly explained by Q, the accumulated FWF* amounts to ~10 % of the accumulated Q with opposite sign. The air-sea buoyancy flux ~~atmospheric forcing estimated in terms of buoyancy~~ is ~~therefore~~ 10% lower on average than ~~when estimated in terms~~

~~of~~the air-sea heat flux. Considering the Ekman transports, the 1993 – 2018 means of the accumulated BF_{ek}, HF_{ek} and SF_{ek} from 1 September to 31 March amount to 0.37 ± 1.15 x 10^8 J m^{-2}, -0.35 ± 1.36 x 10^8 J m^{-2}, and 0.02 ± 2.04 x 10^8 x 10^9 J m^{-2}, respectively. The horizontal Ekman heat flux is negative, while the Ekman buoyancy flux is positive. This buoyancy gain indicates a southeastward transport of surface freshwater caused by dominant winds from the southwest. Noteworthy, BF_{ek} is one order of magnitude smaller than the B_{surf}*.

~~Piron et al. (2016) found that "the wind stress led to an Ekman-induced heat loss that reinforced by about 10% the heat loss induced by the net air-sea heat fluxes". Here, we considered the buoyancy flux induced by the Ekman response to the wind stress and we estimated the buoyancy, heat and salt Ekman fluxes (BF_{ek}, HF_{ek} and SF_{ek}). The means (1993 – 2018) of the accumulated BF_{ek}, HF_{ek} and SF_{ek} from 1 September to 31 March amount to – 0.0004 ± 0.04 x 10^9 J m^{-2}, 0.0446 ± 0.04 x 10^9 J m^{-2}, and 0.0626 ± 0.04 x 10^9 J m^{-2}, respectively. So, on average, HF_{ek} and SF_{ek} compensate each other resulting in an almost zero J m^{-2} BF_{ek}. However, for particular years with strong wind stress as it was the case in 2015, there is no such compensation and BF_{ek} is different from 0 (see Fig. 4).~~

~~We now compare the accumulated B_{surf}* from 1 September to 31 March the year after for the last four deep convection years. It amounted to - 3.21 x 10^9 ± 0.05 J m^{-2}, - 2.29 ± 0.04 x 10^9 J m^{-2}, - 2.23 ± 0.05 x 10^9 J m^{-2} and - 2.58 ± 0.05 x 10^9 J m^{-2} for W2015, W2016, W2017 and W2018, respectively. The cumulative sum of BF_{ek} from 1 September 2014 to 31 March 2015 was - 0.27 ± 0.04 x 10^9 J m^{-2}; the estimates for the following winters were near 0 J m^{-2}. When the BF_{ek} is added to the B_{surf}*, the resulting atmospheric forcing is - 3.48 x 10^9 ± 0.05 J m^{-2}, - 2.19 ± 0.04 x 10^9 J m^{-2}, - 2.20 ± 0.05 x 10^9 J m^{-2} and - 2.57 ± 0.05 x 10^9 J m^{-2} for W2015, W2016, W2017 and W2018, respectively. The estimate for W2015 is ~30% larger than the estimates for 2016 – 2018. Time series of atmospheric forcing anomalies in Fig. 4 show that this strongly negative W2015 anomaly of accumulated B_{surf}* was caused by very negative Q and FWF anomalies and a negative BF_{ek} as well. During W2016, W2017 and W2018 however, all atmospheric forcing terms were close to zero.~~

The total atmospheric forcing SECF was quantified as the sum of B_{surf}* and BF_{ek}. The anomalies of accumulated fluxes from 1 September to 31 August the year after, with respect to the mean 1993 – 2016, are displayed in Fig. 4 for the SECF box. The grey line in Fig. 4a is the total atmospheric forcing anomaly (B_{surf}* plus BF_{ek}). We identify years with very negative buoyancy loss in the SECF region, e.g. 1994, 1999, 2008, 2012 and 2015. The very negative anomalies of atmospheric forcing in 1999 and 2015 were caused by the very negative anomalies in both B_{surf}* (Fig. 4a) and BF_{ek} (Fig.4d). This correlation was not observed for all the years presenting a negative anomaly of atmospheric forcing.

Noteworthy, during W2016, W2017 and W2018, the anomaly of atmospheric forcing was close to zero.

~~From these results we conclude that, c~~Contrary to the very negative anomaly in atmospheric fluxes over the ~~Irminger Sea~~SECF region observed for W2015, the atmospheric fluxes were close to the mean during W2016, W2017 and W2018.

4.3. Analysis of the preconditioning of the water column ~~in the Irminger Sea~~SouthEast of Cape Farewell

Our hypothesis is that the exceptional deep convection that happened in W2015 in the Irminger Sea favorably preconditioned the water column for deep convection the following winters. The time-evolution of θ, S, σ_1 and of $\Delta\sigma_1$=0.01 kg m^{-3} layer thicknesses (Fig. 5) show a marked change in the hydrological properties of the Irminger Sea at the beginning of 2015 caused by the exceptional deep convection that occurred during W2015 (see also Piron et al., 2017). The intermediate waters (500 – 1,000 m) became colder than the years before and, despite a slight decrease in salinity, the cooling caused the density to increase (Fig. 5c). Fig. 5d shows $\Delta\sigma_1$=0.01 kg m^{-3} layer thicknesses larger than 600 m appearing at the end of W2015 for the first time since 2002. In the density range 32.36 – 32.39 kg m^{-3}, these layers remained thicker than ~450 m during W2016 to W2018. This indicates low stratification at intermediate depths and a favorable preconditioning of intermediate waters for deep convection due to W2015 deep convection. The denser density of the core of the thick layers in 2017 -2018 compared with 2015 - 2016 agrees with the densification of the mixed layer SECF shown in Table 1 and Fig. 3.

B(zi) is our estimate of the preconditioning of the water column before winter (see Method). Fig. 6a shows that, deeper than 100 m, B ~~was smaller~~ for W2016, W2017 and W2018 was smaller than for W2015 or B for the mean W2008 – W2014. Furthermore, for W2016, W2017 and 2018, B remained nearly constant with depth between 600 and 1,300 m, which means that once the water column has been homogenized down to 600 m, little additional buoyancy loss results in homogenization of the water column down to 1,300 m. Both conditions (i) less buoyancy to be removed and (ii) absence of gradient in the B profile down to 1,300 m indicate a more favorable preconditioning of the water column for W2016, W2017 and W2018 than during W2008 – W2015.

To understand the relative contributions of θ and S to the preconditioning, we computed the thermal (B_θ) and haline (B_S) components of B ($B = B_\theta + B_S$). In general, B_θ (B_S) increases with depth when θ decreases (S increases) with depth. On the contrary, a negative slope in B_θ (B_S) profile corresponds to

θ increasing (S decreasing) with depth and is indicative of a destabilizing effect. The negative slopes in B_θ and B_s profiles are not observed simultaneously because density profiles are stable.

We describe the relative contributions of B_θ and B_s to B by looking first at the mean 2008 – 2014 profiles (discontinuous blue lines in Fig. 6). B_θ accounts for most of the increase in B from the surface to 800 m and below 1,400 m (see Fig. 6a and Fig. 6b). The negative slope in the B_s profile between 800 – 1,000 m (Fig. 6b) slightly reduces B (Fig. 6a) and is due to the decrease in S associated with the core of LSW (see Fig. 3 in Piron et al. 2016). In the layer 1,000 – 1,400 m, the increase in B (Fig. 6a) is mainly explained by the increase in B_s (Fig. 6b), which follows the increase in S in the transition from LSW to Iceland Scotland Overflow Water (ISOW). This transition layer ~~that~~ will be referred to hereinafter as the deep halocline. The evaluation of the preconditioning of the water column was usually analyzed in terms of heat (e.g., Piron et al. 2015; 2017). The decomposition of B in B_θ and B_S reveals that θ governs B in the layer 0 – 800 m. S tends to reduce the stabilizing effect of θ in the layer 800 – 1,000 m, and reinforces it in the layer 1,000 – 1,400 m in adding up to 1 x 10^9 J m^2 to B.

In order to further understand why the Irminger Sea was favorably preconditioned during winters 2016 – 2018, we compare the B_θ and B_S of W2017, which was the most favorably preconditioned winter, with the mean 2008 – 2014 (Fig. 7a). From the surface to 1,600 m, B_θ and B_S were smaller for W2017 than for the mean 2008 – 2014. There are two additional remarkable features. First, in the layer 500 – 1000 m, the large reduction of B_θ, in relation to its mean 2008 – 2014, mostly explains the decrease of B in this layer. Second, the more negative value of B_s in the layer 1,100 – 1,300 m, compared to its mean 2008 – 2014, eroded the B_θ slope, making the B profile more vertical for W2017 than in the mean. The more negative contribution of B_s in the layer 1,100 – 1,300 m ~~is related to~~comes from the fact that the deep halocline was deeper for W2017 (1,300 m, see ~~red~~ orange dashed~~discontinuous~~ line in Fig. 7a) than for the mean 2008 – 2014 (1,000 m, see blue dashed~~discontinuous~~ line in Fig. 7a). Finally, we note that the profiles of $B(z_i)$, $B_\theta(z_i)$ and $B_s(z_i)$ for W2016 and W2018 are more similar to the profiles of W2017 than to those of W2015 or to the mean 2008 – 2014 (see Fig. 6), which indicates that the water column was also favorably preconditioned for deep convection in W2016 and W2018 for the same reasons than in W2017.

The origin of the changes in B is now discussed from the time evolutions of the monthly anomalies of θ, S and σ_0 at 58°N – 40°W that is at the center of the SECF box (Fig. 8). The time evolutions there are similar to those at any other location inside the SECF box~~a point in the Irminger Sea (59°N – 40°W, Fig. 8)~~. These anomalies were computed using ISAS (Gaillard et al., 2016) and were referenced to the monthly mean of 2002 – 2016. A positive anomaly of σ_0 appeared in ~~2015~~ 2014 between the surface and 600 m (Fig. 8a) and reached ~~1,100~~1,200 m in ~~2016~~ 2015 and beyond. This positive anomaly of σ_0

correlates with a negative anomaly of θ. The latter ~~that~~, however, reached ~1,400 m depth in 2016 that is deeper than the positive anomaly of σ_0. The negative anomaly of S between 1,000 - 1,500 m that appeared in 2015 and strongly reinforced in 2016 caused the negative anomaly in σ_0 between 1,200 – 1,500 m (the density anomaly caused by the negative anomaly in θ between 1,200 – 1,400 m does not balance the density anomaly caused by the negative anomaly of S).~~started in 2016 caused the negative anomaly in σ_θ between 1,200 – 1,500 m (the negative anomaly in θ between 1,200 – 1,400 m does not balance the negative anomaly of S).~~

The θ and S anomalies in the water column during 2016 – 2018 explain the anomalies of B, B_θ and B_s and can be summarized as follows. On the one hand, the properties of the surface waters (down to 500 m) were colder than previous years and, despite they were also fresher, they were denser. The density increase in the surface water reduced the density difference with the deeper-lying waters. The intermediate layer (500 – 1000 m) was also favorably preconditioned due to the observed cooling. Additionally, in the layer 1,100 – 1,300 m, the large negative contribution of B_s ~~in relation~~with restpect to its mean is explained by the decrease in S in this layer, which caused a decrease in σ_0 and, consequently, reduced the σ_0 difference with the shallower-lying water. The decrease in S also resulted in a deepening of the deep halocline.

4.4. Atmospheric forcing versus preconditioning of the water column

We now use the estimates of the accumulated atmospheric forcing (B_{surf}* + BF_{ek}) from 1 September to 31 March the year after (see Fig. S4) to predict the maximum convection depth for a given winter based on September profiles of B. The predicted convection depth is determined as the depth at which B(zi) (Fig. 6a) equals the accumulated atmospheric forcing. The associated error was estimated by propagating the error in the atmospheric forcing (0.05 x 10^9 J m^{-2}). The accumulated atmospheric forcing amounted to -3.21 x 10^9 ± 0.05 J m^{-2}, -2.21 ± 0.04 x 10^9 J m^{-2}, -2.01 ± 0.05 x 10^9 J m^{-2} and -2.47 ± 0.05 x 10^9 J m^{-2} for W2015, W2016, W2017 and W2018, respectively. We found predicted convection depths of 1,085 ± 20 m, 1,285 ± 20 m, 1,415 ± 20 m and 1,345 ± 20 m for W2015, W2016, W2017 and W2018, respectively. We consider Q3 as the observed estimate of the MLD (Table 1). The predicted MLD agrees with the observed MLD within ± 200 m. The differences could be due to errors in the atmospheric forcing (Josey et al., 2018), lateral advection and/or spatial variation in the convection intensity within the box not captured by the Argo sampling. ~~of atmospheric forcing (B_{surf}* + BF_{ek}) to predict the maximum convection depth for a given winter based on September profiles of B. The predicted convection depths are determined as the depth at which B(zi) equals the atmospheric forcing. The associated error was estimated considering the error in the atmospheric forcing (0.05 x 10^9 J m^{-2}). We found predicted convection depths of 1175 ± 10 m, 1270 ± 25 m, 1425 ±~~

~~10 m and 1285 ± 20 m for W2015, W2016, W2017 and W2018, respectively. The Q3 estimated from W2016 and W2017 observations (1,325 m and 1,400 m, respectively) are very close to the predicted convection depth. In W2015, the predicted convection depth was underestimated compared to the observed Q3 (1,310 m). The contrary is observed for W2018; this result is in line with the fact that Q3 in W2018 was most likely underestimated since 6 out of the 10 profiles from which deep convection was recorded dived down to 1,100 m, which coincided with their MLD. When these 6 profiles are excluded of the analysis, Q3 is 1,300 m, which is within the error bar of the predicted convection depth.~~

The satisfactory predictability of the convection depth with our 1-D model~~validates our neglect of the horizontal advection and~~ indicates that deep convection occurred locally. ~~Finally, this demonstrates that~~ In spite the atmospheric forcing was close to mean (1993 – 2016) conditions during W2016, W2017 and W2018, convection depths > 1300 m were reached in the SECF region. This~~, which~~ was only possible thanks to the favorable preconditioning.

5. DISCUSSION

Deep convection happens in the Irminger Sea and South of Cape Farewell during specific winters because of strong atmospheric forcing (high buoyancy loss), favorable preconditioning (low stratification) or both at the same time (Pickart et al., 2003). In the Irminger Sea, ~~S~~strong atmospheric forcing explained for instance the very deep convection (reaching depth greater than 1500 m) observed in the early 90s (Pickart, et al., 2003) and in W2015 (de Jong et al. 2016; Fröb et al., 2016; Piron et al. 2017)~~., and~~ It explained as well the return of deep convection ~~after many years without convection~~ in W2008 (Väge et al., 2009) and in W2012 (Piron et al., 2016). The favorable preconditioning caused by the densification of the ~~convected layer at the end of~~ mixed layer during W2008 favored a new deep convection event in W2009 despite neutral atmospheric forcing (de Jong et al. 2012). Similarly, the preconditioning observed after W2015 in the SECF region favored deep convection in W2016 (this work). ~~Our study reveals that the preconditioning surprisingly persisted along~~ The favorable preconditioning persisted three consecutive winters (2016 – 2018) in the SECF region, which allowed deep convection although atmospheric forcing was close to the climatological values. Why did this favorable preconditioning persist in time?

~~The favorable preconditioning of the water column during 2016 – 2018 in the Irminger Sea resulted from~~ We previously showed that during 2016 – 2018 two hydro~~lo~~graphic~~ical~~ anomalies affected~~ing~~ different ranges of the water column in SECF region: ~~the~~a cooling ~~of~~intensified in the layer 200 – 800 m and ~~the~~ a freshening ~~of 1,200 – 1,400 m layer~~intensified in 1,000 – 1,500 m layer. Those resulted in

a decrease in the vertical density gradient between the intermediate and the deeper layers creating a favorable preconditioning of the water column. Note that~~,~~ the cooling affected the layer from surface ~~–~~to 1,400 m and the freshening affected the layer from near surface to ~~1,000 – 1,500~~1,600 m ~~(Fig. 8)~~, but the cooling and the freshening were intensified at different depth ranges (Fig. 8). ~~the θS anomalies were density compensated in the layer 1,000 – 1,200 m.~~

We see in Fig. 5a a sudden decrease in θ ~~–~~in the intermediate layers in 2015 compared to the previous years. It indicates that the decrease in θ of the ~~layer 200 – 800 m~~intermediate layer likely originated locally during W2015 when extraordinary deep convection happened. A slight freshening of the water column (400- 1,500 m) appeared in 2015, likely caused by the W2015 convection event, then it decreased before a second S anomaly intensified in 2016 between 1,100 and 1,400 m (Fig. 8c). It is unlikely that this second anomaly was exclusively locally formed by deep convection because it intensified during summer 2016.~~The freshening of the layer 1,200 – 1,400 m appeared in 2016 (Fig. 8c). Given its depth range, it is unlikely that this anomaly was locally formed. Moreover, this anomaly is different to that affecting the intermediate layer because density increased in the intermediate layer with respect to the mean 2002 – 2016, while it decreased in the 1,200 – 1,400 m layer (Fig. 8a).~~ Our hypothesis is that this~~e~~ S anomaly originated in the Labrador Sea and was further transferred to the ~~Irminger Sea~~SECF region by the cyclonic circulation encompassing the Labrador Sea and Irminger Sea at these depths (Daniault et al., 2016; Ollitrault & Colin de Verdière, 2014; Lavander et al., 2000 ; Straneo et al., 2003). It is corraborated by the 2D evolution of the anomalies in S in the layer 1,200 – 1,400 m (Fig. 9): a negative anomaly in S appeared in the Labrador Sea in February 2015, which was transferred southward and northeastward in February 2016 and intensified over the whole SPNA in February 2017. By this mechanism, the advection from the Labrador Sea contributed to create property anomalies in the water column. However, the buoyancy budget showed that this was a minor contribution compared to the buoyancy loss due to the local air-sea flux, even if it was essential to preconditioning the water column for deep convection.

We now compare the atmospheric forcing and the preconditioning of the water column in the ~~Irminger Sea~~ SECF region with those of the nearby Labrador Sea where deep convection happens ~~each~~ almost every year. ~~As noted by Pickart et al. (2003), t~~The atmospheric forcing over the Labrador Sea is ~15 % larger than that over the ~~Irminger Sea~~SECF region: the means (1993 - 2018) of the atmospheric forcing, defined as the time ~~–~~accumulated B_{surf}* + BF_{ek} from 1 September to 31 March the year after, are -2.61 ± 0.55 x 10^9 J m^{-2} in the Labrador Sea and -2.18 ± 0.54 ~~-2.26 ± 0.58~~ x 10^9 J m^{-2} in the ~~Irminger Sea~~SECF region. The difference was larger during the period 2016 – 2018 when the atmospheric forcing equaled -3.10 ± 0.19 x 10^9 J m^{-2} in the Labrador Sea and -2.23 ± 0.23 ~~-2.31 ± 0.21~~ x 10^9 J m^{-2} in the ~~Irminger Sea~~SECF region. In terms of preconditioning, the 2008 – 2014 mean B

profile (blue continuous lines in Fig. 7) was lower by ~0.5 x 10^9 J m^{-2} in the Labrador Sea than ~~in the Irminger Sea~~SECF for the surface to 1,000 m layer and by more than 1 x 10^9 J m^{-2} below ~~1,000~~1,200 m. It indicates that the water column was more favorably preconditioned in the Labrador Sea than in the ~~Irminger Sea~~SECF region during 2008 - 2014. Differently, B for W2017 shows slightly lower values from the surface to 1,300 m in the ~~Irminger Sea~~SECF region than in the Labrador Sea (see orange lines in Fig. 7). However, B in the Labrador Sea remains constant down to the depth of the deep halocline between LSW and North Atlantic Deep Water (NADW) at 1,700 m. In the ~~Irminger Sea~~SECF region, the deep halocline remained at ~1,300 m between 2016 and 2018 (see B_s lines in Fig. 7a). Differently, in the Labrador Sea, the deep halocline ~~was successive~~ deepen~~ed~~ing from 1,200 m for the mean to 1,735 m, 1,775 m and 1905 m in W2016, W2017 and W2018, respectively (see ~~discontinuous~~ dashed lines in Fig. 7b). The deep halocline acts as a physical barrier for deep convection in both the ~~Irminger Sea~~SECF region and the Labrador Sea, but because it is deeper in the Labrador Sea than in the ~~Irminger Sea~~SECF region, ~~-~~the preconditioning is more favorable to a deeper convection in the Labrador Sea than in the SECF region~~a deeper convection depth is granted in the former than in the latter~~. Summarizing, ~~the atmospheric forcing and the preconditioning of the water column are in general more favorable for deep convection in the Labrador Sea than in the Irminger Sea. In~~in winters 2016 - 2018 in the Labrador Sea, both atmospheric forcing and preconditioning of the water column ~~favored by a deeper than average deep halocline,~~ granted the deepest convection depth ~~ever observed~~ in the Labrador Sea since the beginning of the Argo period (comparison of our results with those of Yashayaev and Loader, 2017). Contrasting, in the ~~Irminger Sea~~SECF region, during the same period, the atmospheric forcing was close to climatological values, and the favorable preconditioning of the water column allowed 1,300 m depth convection, what was exceptional for the ~~Irminger Sea~~SECF region.

The Labrador Sea, SECF region and Irminger Sea are three distinct deep convection sites (e.g. Yashayaev et al., 2007; Bacon et al., 2003; Pickart et al., 2003; Piron et al., 2017). In this work, we give new insights on the connections between the different sites, showing how lateral advection of fresh LSW formed in the Labrador Sea favored the preconditioning in the SECF region fostering deeper convection.

~~In the following we consider the time – evolution of θ, S and σ_θ at the layer 700 – 900 m (Fig. 10), considered here as the core of the LSW in both the Irminger Sea and the Labrador Sea. From 2002 to 2012, a progressive increase in the θ and S of the LSW core in the Irminger Sea is noticeable despite the high frequency variability. The θ and S changes were not density compensated causing a decadal decrease in σ_θ of ~0.01 Kg m^{-3}. From 2012 to 2015, both θ and S decreased, while σ_θ remained~~

~~constant. During 2015 – 2018, θ decreased from 3.6 °C to 3.2 °C, and σ_θ increased from 27.72 to 27.75 kg m^{-3} (see also Fig. 3 and Table 1). In spite of the cooling and densification that occurred during the last winters, LSW is warmer and lighter than that formed during W1994 and W1995 (2.85°C, 27.78 kg m^{-3}, Pickart et al. 2003). We note a long-term (1994 – 2018) warming of LSW observed in the Irminger Sea. The comparison with the LSW properties in the Labrador Sea over 2002 – 2018 (Fig. 9) shows that the LSW observed in both basin has the same density while that of the Irminger Sea is warmer and saltier than that of the Labrador Sea. Interestingly, this behaviour was also observed along the 90s (Pickart et al, 2003). It is also worth noting that θ and S observed in Labrador Sea and Irminger Sea converged at the end of the 90s (Fig. 6 in Pickart et al., 2003) and along our period 2015 – 2018 (Fig. 3 and Fig. 10). However, there is an imporant difference between the two periods: deep convection was not observed in the Irminger Sea at the end of the 90s while it was very intense during 2015 – 2018. This disparity might indicate that Labrador Sea and Irminger Sea are evolving differentely and only further observations would disclose the origin and mechanisms causing the differences.~~

Climate models forecast increasing input of freshwater in the North Atlantic due to ice-melting under present climate change (B~~r~~amber et al., 2018), which could reduce, or even shut-down, the deep convection in the North Atlantic (Yang et al., 2016; Brodeau & Koenigk, 2016). We observed a fresh anomaly in the surface waters in regions close to the eastern coast of Greenland in 2016 that extended to the whole Irminger Sea in 2017 (Fig. ~~S4~~S6). However, ~~at the moment, the~~this surface freshening did not hamper the deep convection in ~~the Irminger Sea~~SECF region possibly because the surface water also cooled~~, which favors the preconditioning for deep convection~~. Swingedouw et al., 2013 indicated that the freshwater signal due to Greenland ice sheet melting is mainly accumulating in the Labrador Sea. However, no negative anomaly of S was detected in the surface waters of the Labrador Sea (Fig. ~~S4~~S6). It might be explained by the intense deep convection affecting the Labrador Sea since 2014 that could have transferred the surface freshwater anomaly to the ocean interior. This suggest that, in the last years, the interactions between expected climate change anomalies and the natural dynamics of the system combined to favor very deep convection. This however does not foretell the long term response to climate change.

6. CONCLUSIONS

During 2015 – 2018 winter deep convection happened in the ~~Irminger Sea~~SECF region reaching deeper than 1,300 m. It is the first time deep convection was observed in ~~the Irminger Sea~~this region

during four consecutive winters. ~~LSW formed in the Irminger Sea from 2015 to 2018 get colder, fresher and denser, being similar in 2018 to the properties of the LSW formed in the Labrador Sea.~~

~~Considering the expected increase in freshwater inputs, the atmospheric forcing and preconditioning of~~ The atmospheric forcing and preconditioning of the water column was evaluated in terms of buoyancy. We showed that the atmospheric forcing is 10% weaker when evaluated in terms of buoyancy than in terms of heat because of the non-negligible effect of the freshwater flux. The analysis of the preconditioning of the water column in terms of buoyancy to be removed (B) and its thermal and salinity terms (B_θ and B_s) revealed that B_θ dominated the B profile from the surface to 800 m and B_s reduced the B in the 800 – 1000 m layer because of low salinity of LSW. Deeper, B_s increased B due to the deep halocline (LSW-ISOW) that acted as a physical barrier limiting the depth of the convection.

During 2016 – 2018, the air-sea buoyancy losses were close to the climatological values and the very deep convection was possible thanks to the favorable preconditioning of the water column. It was surprising that these events reached convection depths similar to those observed in W2012 and W2015, when the latter were provoked by high air-sea buoyancy loss intensified by the effect of strong wind stress. It was also surprising that the water column remained favorably preconditioned during three consecutive winters without strong atmospheric forcing. In this paper, we studied the reasons why this happened.

The ~~favorable~~ preconditioning for deep convection during 2016 – 2018 was particularly favorable due to the combination of two types of ~~hydrological~~ hydrographic anomalies affecting different depth ranges. First, the surface and intermediate waters (~~200 –~~down to 800 m) were~~as~~ favorably preconditioned because buoyancy (density) decreased (increased) due to the cooling caused by the deep convection of W2015. Second, buoyancy (density) increased (decreased) in the layer 1,200 – 1,400 m due to the decrease in S caused by the lateral advection of fresher LSW formed in the Labrador Sea. The S anomaly of this layer resulted in a deeper deep halocline. Hence, the cooling of the intermediate water was essential to reach convection depth of 800 – 1,000 m, and the freshening in the layer 1,200 – 1,400 m and the associated deepening of the deep halocline, allowed the very deep convection (> 1,300 m) in W2016 – W2018.

Author contribution: PZ treated and analyzed the data. PZ and HM interpreted the results. PZ, HM and VT discussed the results and wrote the paper.

ACKNOWLODGEMENT

The Argo data were collected and made freely available by the International Argo Program and the national programs that contribute to it. (http://www.argo.ucsd.edu, http://argo.jcommops.org). The Argo Program is part of the Global Ocean Observing System. The NAO data were downloaded from the UCAR Climate Data Guide website (Schneider et al., 2013): https://climatedataguide.ucar.edu/climate-data/hurrell-north-atlantic-oscillation-nao-index-pc-based. The Ssalto/Duacs altimeter products were produced and distributed by the Copernicus Marine and Environment Monitoring Service (CMEMS) (http://www.marine.copernicus.eu).

REFERENCES

Argo Data Management Team: Argo user's manual V3.2. https://doi.org/10.13155/29825, 2017

Argo group: Argo float data and metadata from Global Data Assembly Centre (Argo GDAC), SEANOE, https://doi.org/10.17882/42182 ,2019

Bacon, S.: Circulation and Fluxes in the North Atlantic between Greenland and Ireland. *Journal of Physical Oceanography*, *27*(7), 1420–1435. *https://doi.org/10.1175/1520-0485(1997)027<1420:CAFITN>2.0.CO;2*, 1997.

Bacon, S., Gould, W. J. and Jia, Y.: Open-ocean convection in the Irminger Sea, Geophys. Res. Lett., 30(5), 1246, doi:10.1029/2002GL016271, 2003.

Bamber, J. L., Tedstone, A. J., King, M. D., Howat, I. M., Enderlin, E. M., van den Broeke, M. R., & Noel, B.: Land Ice Freshwater Budget of the Arctic and North Atlantic Oceans: 1. Data, Methods, and Results, *Journal of Geophysical Research: Oceans*, 1–11, https://doi.org/10.1002/2017JC013605, 2018.

Billheimer, S., & Talley, L. D.: Near cessation of Eighteen Degree Water renewal in the western North Atlantic in the warm winter of 2011 – 2012, *118*(November), 6838–6853, https://doi.org/10.1002/2013JC009024, 2013.

Brodeau, L., & Koenigk, T.: Extinction of the northern oceanic deep convection in an ensemble of climate model simulations of the 20th and 21st centuries, *Climate Dynamics*, *46*(9–10), 2863–2882. https://doi.org/10.1007/s00382-015-2736-5, 2016.

Centurioni and Gould, W. J.: Winter conditions in the Irminger Sea observed with profiling floats, *Journal of Marine Research*, 62, 313–336, 2004.

Daniault, N., Mercier, H., Lherminier, P., Sarafanov, A., Falina, A., Zunino, P., Gladyshev, S. : The northern North Atlantic Ocean mean circulation in the early 21st century, *Progress in Oceanography*, *146*(June), 142–158, https://doi.org/10.1016/j.pocean.2016.06.007, 2016.

de Boyer Montégut, C., Madec, G., Fischer, A. S., Lazar, A., & Iudicone, D.: Mixed layer depth over the global ocean: An examination of profile data and a profile-based climatology, *Journal of Geophysical Research C: Oceans*, *109*(12), 1–20, https://doi.org/10.1029/2004JC002378, 2004.

de Jong, M.F., Oltmanns, M., Karstensen, J., and de Steur, L.: Deep Convection in the Irminger Sea Observed with a Dense Mooring Array, *31*(February), 50–59, https://doi.org/10.5670/oceanog.2018.109, 2018.

de Jong, M. F., & de Steur, L.: Strong winter cooling over the Irminger Sea in winter 2014–2015, exceptional deep convection, and the emergence of anomalously low SST, *Geophysical Research Letters*, *43*(13), 7106–7113. https://doi.org/10.1002/2016GL069596, 2016.

De Jong, M. F., Van Aken, H. M., Våge, K., & Pickart, R. S.: Convective mixing in the central Irminger Sea: 2002-2010, *Deep-Sea Research Part I: Oceanographic Research Papers*, *63*, 36–51. https://doi.org/10.1016/j.dsr.2012.01.003, 2012.

Dee, D. P., Uppala, S. M., Simmons, A. J., Berrisford, P., Poli, P., Kobayashi, S., Vitart, F.: The ERA-Interim reanalysis: Configuration and performance of the data assimilation system, *Quarterly Journal of the Royal Meteorological Society*, *137*(656), 553–597. https://doi.org/10.1002/qj.828, 2011.

Fröb, F., Olsen, A., Våge, K., Moore, G.W.K., Yashayaev, I., Jeansson, E. & Rajasakaren B.: Irminger Sea deep convection injects oxygen and anthropogenic carbon to the ocean interior. NATURE COMMUNICATIONS | 7:13244 | DOI:10.1038/ncomms13244|www.nature.com/naturecommunications, 2016.

Gaillard, F., Reynaud, T., Thierry, V., Kolodziejczyk, N., & Von Schuckmann, K.: In situ-based reanalysis of the global ocean temperature and salinity with ISAS: Variability of the heat content and steric height. *Journal of Climate*, *29*(4), 1305–1323. https://doi.org/10.1175/JCLI-D-15-0028.1, 2016.

Gill, A. E. (1982), Atmosphere-Ocean Dynamics, vol. 30, Academic, San Diego, CA.

Good, S. A., Martin, M. J., & Rayner, N. A.: EN4: Quality controlled ocean temperature and salinity profiles and monthly objective analyses with uncertainty estimates. *Journal of Geophysical*

Research: Oceans, *118*(12), 6704–6716. https://doi.org/10.1002/2013JC009067, 2013.

~~IPCC: Climate Change 2013: The Physical Science Basis. Contribution of Working Group I to the Fifth Assessment Report of the Intergovernmental Panel on Climate Change [Stocker, T.F., D. Qin, G.-K. Plattner, M. Tignor, S.K. Allen, J. Boschung, A. Nauels, Y. Xia, V. Bex and P.M. Midgley (eds.)]. Cambridge University Press, Cambridge, United Kingdom and New York, NY, USA, 1535 pp, 2013.~~

Josey, S. A., Hirschi, J. J.-M., Sinha, B., Duchez, A., Grist, J. P., Marsh, R.: The Recent Atlantic Cold Anomaly: Causes, Consequences, and Related Phenomena. Annual Review of Marine Science, 10 (1). 475-501.https://doi.org/10.1146/annurev-marine-121916-063102, 2018

Kieke, D., & Yashayaev, I.: Studies of Labrador Sea Water formation and variability in the subpolar North Atlantic in the light of international partnership and collaboration. *Progress in Oceanography*, *132*, 220–232. https://doi.org/10.1016/j.pocean.2014.12.010, 2015a.

Kieke, D., & Yashayaev, I.: Studies of Labrador Sea Water formation and variability in the subpolar North Atlantic in the light of international partnership and collaboration, *Progress in Oceanography*, *132*, 220–232, https://doi.org/10.1016/j.pocean.2014.12.010, 2015b.

Kolodziejczyk, N., Prigent-Mazella A., and Gaillard F. (2017). ISAS-15 temperature and salinity gridded fields**. SEANOE**. http://doi.org/10.17882/52367

Lavender, K. L.,Davis, R. E., & Owens, W. B.: Mid-depth recirculation observed in the interior Labrador and Irminger seas by direct velocity measurements. NATURE |VOL 407 | 7 SEPTEMBER 2000 |www.nature.com, 2000.

Marshall, J., & Schott, F.: Open-Ocean Convection ' Theory , and Models Observations ,. *Reviews of Geophysics*, *37*(98), 1–64. https://doi.org/10.1029/98RG02739, 1999.

Ollitrault, M., & Colin de Verdière, A.: The Ocean General Circulation near 1000-m Depth, *Journal of Physical Oceanography*, *44*(1), 384–409. https://doi.org/10.1175/JPO-D-13-030.1, 2014.

Pickart, R. S., Straneo, F., & Moore, G. W. K.: Is Labrador Sea Water formed in the Irminger basin? *Deep-Sea Research Part I: Oceanographic Research Papers*, *50*(1), 23–52, https://doi.org/10.1016/S0967-0637(02)00134-6, 2003.

Piron, A., Thierry, V., Mercier, H., & Caniaux, G.: Argo float observations of basin-scale deep convection in the Irminger sea during winter 2011–2012. *Deep-Sea Research Part I: Oceanographic Research Papers*, *109*, 76–90. https://doi.org/10.1016/j.dsr.2015.12.012, 2016.

692 Piron, A., Thierry, V., Mercier, H., & Caniaux, G.: Gyre-scale deep convection in the subpolar North
693 Atlantic Ocean during winter 2014–2015. *Geophysical Research Letters*, *44*(3), 1439–1447.
694 https://doi.org/10.1002/2016GL071895, 2017.

695 ~~Rahmstorf, S., Box, J. E., Feulner, G., Mann, M. E., Robinson, A., Rutherford, S., & Schaffernicht, E. J.:~~
696 ~~Exceptional twentieth-century slowdown in Atlantic Ocean overturning circulation, *Nature*~~
697 ~~*Climate Change*, *5*(5), 475–480. https://doi.org/10.1038/nclimate2554, 2015.~~

698 Rhein, M, Steinfeldt, R, Kieke, D, Stendardo, I and Yashayaev, I.: Ventilation variability of Labrador
699 Sea Water and its impact on oxygen and anthropogenic carbon: a review, *Philosophical*
700 *Transactions of the Royal Society A: Mathematical, Physical and Engineering Sciences*,
701 375(2102). 20160321. doi:10.1098/rsta.2016.0321, 2017.

702 Schmidt, S., & Send, U.: Origin and Composition of Seasonal Labrador Sea Freshwater, *Journal of*
703 *Physical Oceanography*, *37*(6), 1445–1454. https://doi.org/10.1175/JPO3065.1, 2007.

704 Straneo, F, Pickart, R.S., Lavender, K.: Spreading of Labrador sea water: an advective-diffusive study
705 based on Lagrangian data. Deep-Sea Research Part I-Oceanographic Research Papers. 50:701-
706 719, 2003.

707 Swingedouw, D., Rodehacke, C. B., Behrens, E., Menary, M., Olsen, S. M., & Gao, Y.: Decadal
708 fingerprints of freshwater discharge around Greenland in a multi-model ensemble, 695–720.
709 https://doi.org/10.1007/s00382-012-1479-9, 2013.

710 ~~Thomson, R. E., & Fine, I. V.: Estimating mixed layer depth from oceanic profile data, *Journal of*~~
711 ~~*Atmospheric and Oceanic Technology*, *20*(2), 319–329. https://doi.org/10.1175/1520-~~
712 ~~0426(2003)020<0319:EMLDFO>2.0.CO;2, 2003.~~

713 Yang, Q., Dixon, T. H., Myers, P. G., Bonin, J., Chambers, D., & Van Den Broeke, M. R.: Recent
714 increases in Arctic freshwater flux affects Labrador Sea convection and Atlantic overturning
715 circulation, *Nature Communications*, *7*, 1–7. https://doi.org/10.1038/ncomms10525, 2016.

716 Yashayaev, I., Bersch, M., & van Aken, H. M.: Spreading of the Labrador Sea Water to the Irminger
717 and Iceland basins, *Geophysical Research Letters*, *34*(10), 1–8.
718 https://doi.org/10.1029/2006GL028999, 2007.

719 Yashayaev, I., & Clarke, A.: Evolution of North Atlantic Water Masses Inferred From Labrador Sea
720 Salinity Series, *Oceanography*, *21*(1), 30–45. https://doi.org/10.5670/oceanog.2008.65, 2008.

721 Yashayaev, I., & Loder, J. W.: Recurrent replenishment of Labrador Sea Water and associtated

722 decadal-scale variability, *Journal Geophysical Research: Oceans*, *121*, 8095–8114,
723 https://doi.org/10.1002/2016JC012046, 2016.

724 Yashayaev, I., & Loder, J. W.: Further intensification of deep convection in the Labrador Sea in 2016.
725 *Geophysical Research Letters*, *44*(3), 1429–1438. https://doi.org/10.1002/2016GL071668, 2017.

726 ~~Zunino, P., Lherminier, P., Mercier, H., Daniault, N., García-Ibáñez, M. I., & Pérez, F. F.: The GEOVIDE~~
727 ~~cruise in May-June 2014 reveals an intense Meridional Overturning Circulation over a cold and~~
728 ~~fresh subpolar North Atlantic, *Biogeosciences*, *14*(23), 5323–5342. https://doi.org/10.5194/bg-~~
729 ~~14-5323-2017, 2017.~~

730

731 Table 1. Properties of the deep convection ~~in the Irminger Sea~~SECF and in the Labrador Sea in winters
732 2015 – 2018. We show: the maximal MLD observed, the aggregate maximum depth of convection
733 Q3, the σ_0, S and θ of the winter mixed layer formed during the convection event and n, which is the
734 number of Argo profiles indicating deep convection. The uncertainties given with σ_0, S and θ are the
735 standard deviation of the n values considered to estimate the mean values.

SECF	Maximal MLD (m)	Q3 MLD (m)	σ_0	Salinity	θ	n
W2015	1710	1205	27.733 ± 0.007	34.866± 0.013	3.478 ± 0.130	29
W2016	1575	1471	27.746± 0.002	34.871± 0.003	3.388 ± 0.032	3
W2017	1400	1251	27.745± 0.007	34.868± 0.007	3.364± 0.109	3
W2018	1300	1300	27.748± 0.001	34.859± 0.003	3.263± 0.031	2
LABRADOR SEA	Maximal MLD	Q3 MLD	σ_0	Salinity	θ	n
W2015	1675	1504	27.733 ± 0.009	34.842 ± 0.010	3.279 ± 0.036	41
W2016	1801	1620	27.743 ± 0.006	34.836 ± 0.010	3.124 ± 0.047	18

W2017	1780	1674	27.752 ± 0.008	34.853 ± 0.009	3.172 ± 0.029	26
W2018	2020	1866	27.756 ± 0.006	34.855 ± 0.010	3.145 ± 0.083	13
~~**IRMINGER SEA**~~	~~Maximal MLD~~	~~Q3 MLD~~	~~σ_θ~~	~~θ~~	~~Salinity~~	~~n~~
~~**W2015**~~	~~1715~~	~~1310~~	~~27.732 ± 0.007~~	~~3.494 ± 0.139~~	~~34.868 ± 0.015~~	~~37~~
~~**W2016**~~	~~1575~~	~~1325~~	~~27.745 ± 0.004~~	~~3.444 ± 0.150~~	~~34.877 ±0.017~~	~~7~~
~~**W2017**~~	~~1400~~	~~1400~~	~~27.746 ± 0.006~~	~~3.324 ± 0.113~~	~~34.864 ± 0.009~~	~~4~~
~~**W2018**~~	~~1300~~	~~1100/1300*~~	~~27.751 ± 0.007~~	~~3.188 ± 0.058~~	~~34.854 ± 0.013~~	~~10~~
~~**LABRADOR SEA**~~	~~Maximal MLD~~	~~Q3 MLD~~	~~σ_θ~~	~~θ~~	~~Salinity~~	~~n~~
~~**W2015**~~	~~1675~~	~~1504~~	~~27.733 ± 0.009~~	~~3.279 ± 0.036~~	~~34.842 ± 0.010~~	~~41~~
~~**W2016**~~	~~1801~~	~~1620~~	~~27.743 ± 0.006~~	~~3.124 ± 0.047~~	~~34.836 ± 0.010~~	~~18~~
~~**W2017**~~	~~1780~~	~~1674~~	~~27.752 ± 0.008~~	~~3.172 ± 0.029~~	~~34.853 ± 0.009~~	~~26~~
~~**W2018**~~	~~2020~~	~~1866~~	~~27.756 ± 0.006~~	~~3.145 ± 0.083~~	~~34.855 ± 0.010~~	~~13~~

~~*Q3 estimated when the data of Float 5903102 were excluded of the analysis. We exclude them because their MLDs matched with the maximal depth dived by the float.~~

742 **FIGURES**

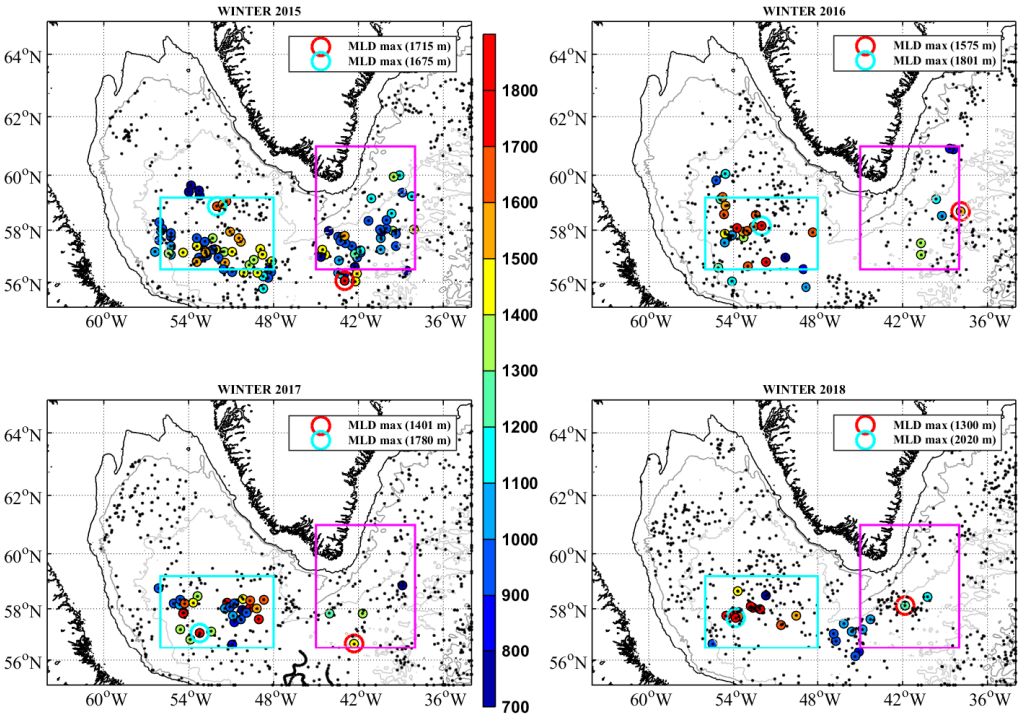

743

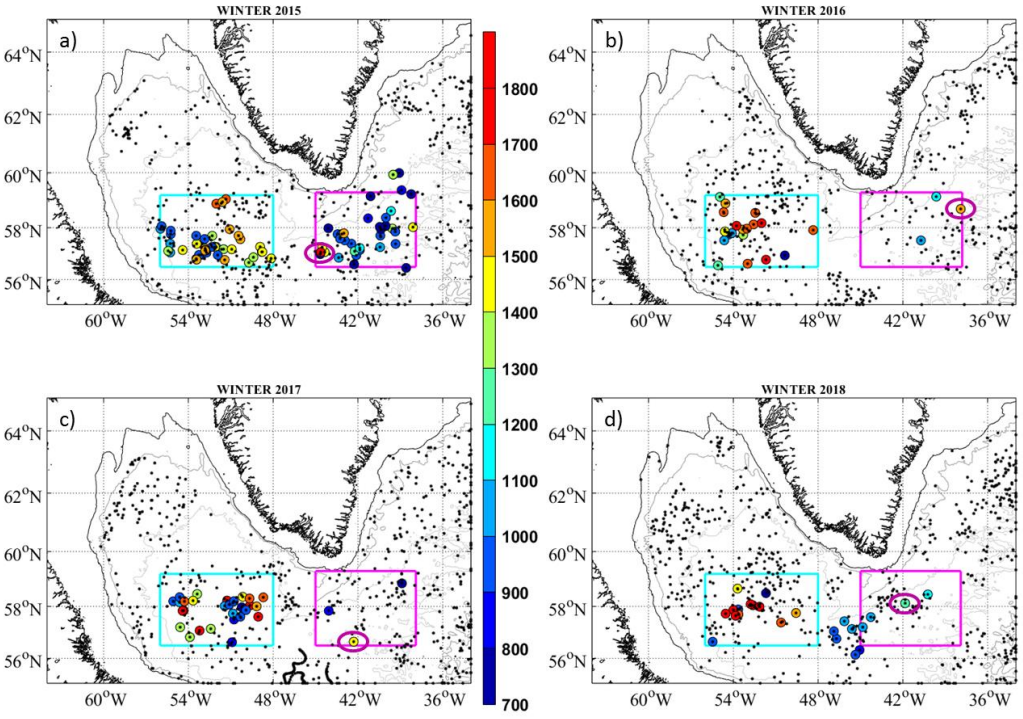

744

745 **Figure 1.** Position of all Argo floats north of 55°N in the Atlantic between 1 January and 30 April a)

746 2015, b) 2016, c) 2017 and d) 2018 (~~small~~ black and colored points). The colored ~~big~~ points and

colorbar indicate the ~~depth of the~~ mixed layer depth (MLD) when MLD deeper than 700 m. ~~, which indicates deep convection.~~ The pink circles ~~correspond to~~indicate the positions of the ~~profiles with the~~ maximumal MLD ~~for the given box~~observed SECF each winter. The pink and cyan boxes delimit the regions used for estimating the time series of atmospheric forcing and the vertical profiles of buoyancy to be removed in the ~~Irminger Sea~~SECF region and Labrador Sea, respectively (Irminger Sea: 56.5°N – ~~61.0~~59.3°N and 45.0°W – 38.0°W, Labrador Sea: 56.5°N – 59.2°N and 56°W – 48°W).

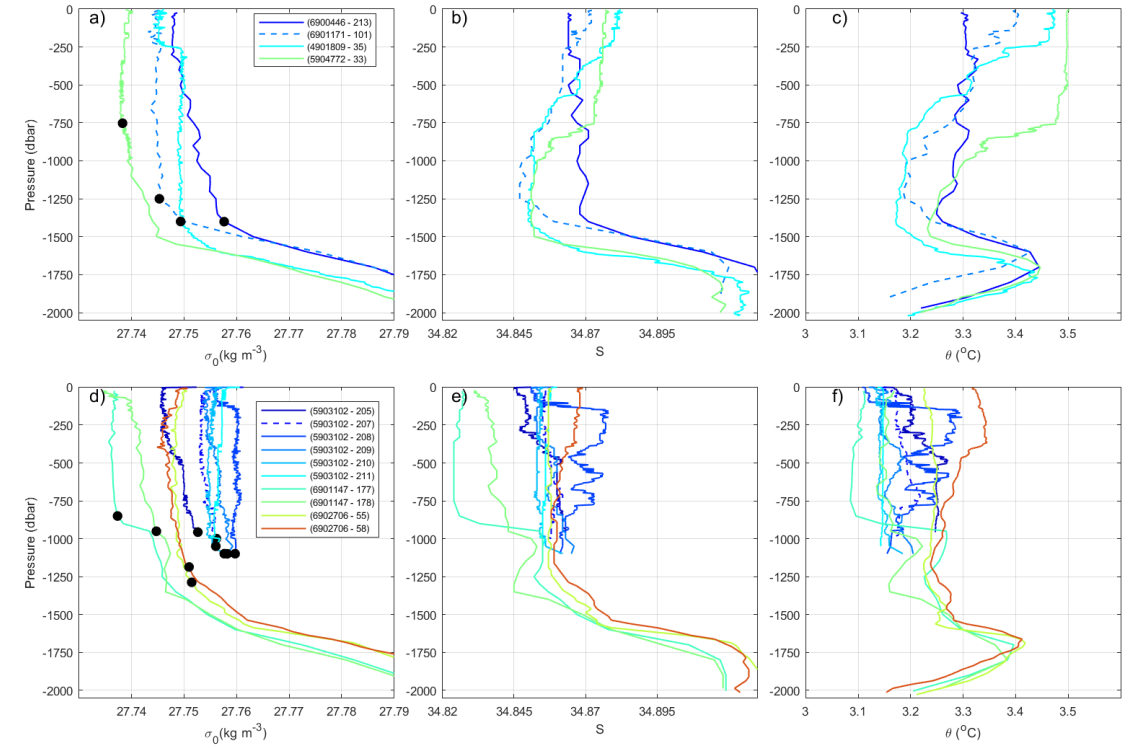

753

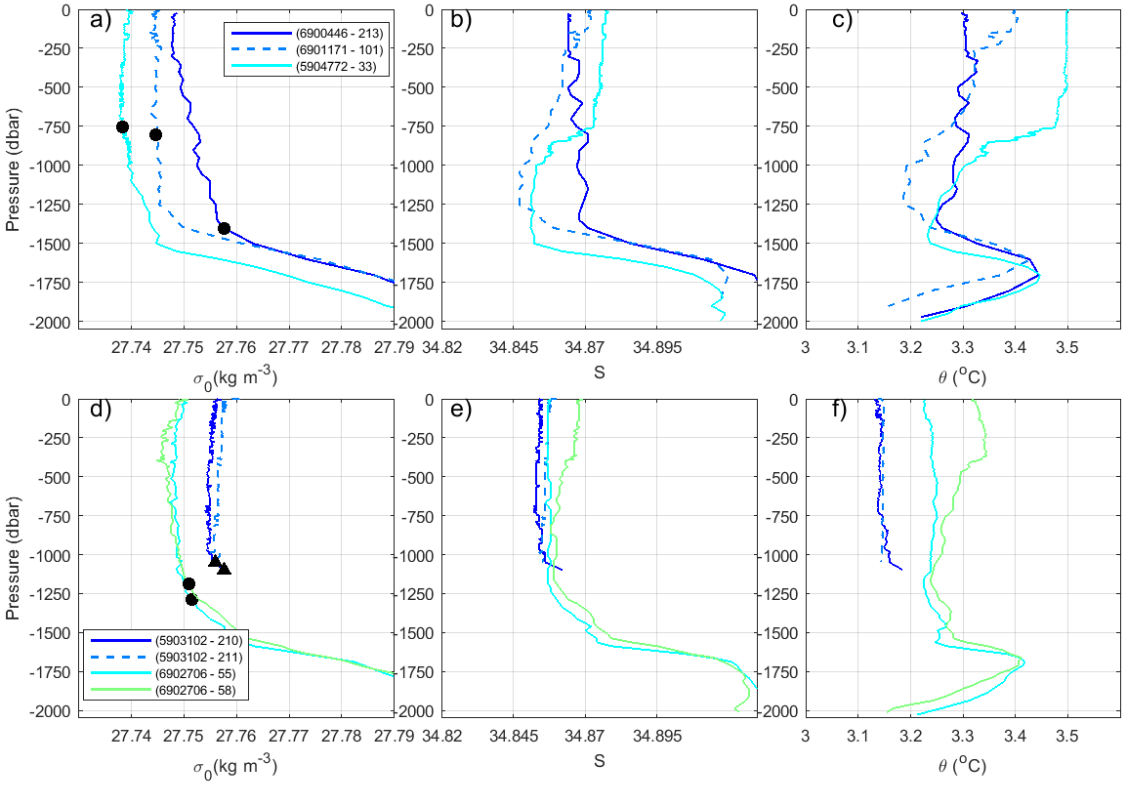

754

755 **Figure 2**. Vertical distribution of σ_0, S and θ of Argo profiles showing MLD deeper than 700 m ~~in the~~
756 ~~Irminger Sea~~SECF in Winter 2017 (a, b and c) and in Winter 2018 (d, e, f). The black points indicate

the MLD ~~in each profile~~. The triangles in d) are the MLD which coincided with the maximal profiling pressure reached by the float. In the legend, the float and cycle of each profile are indicated.

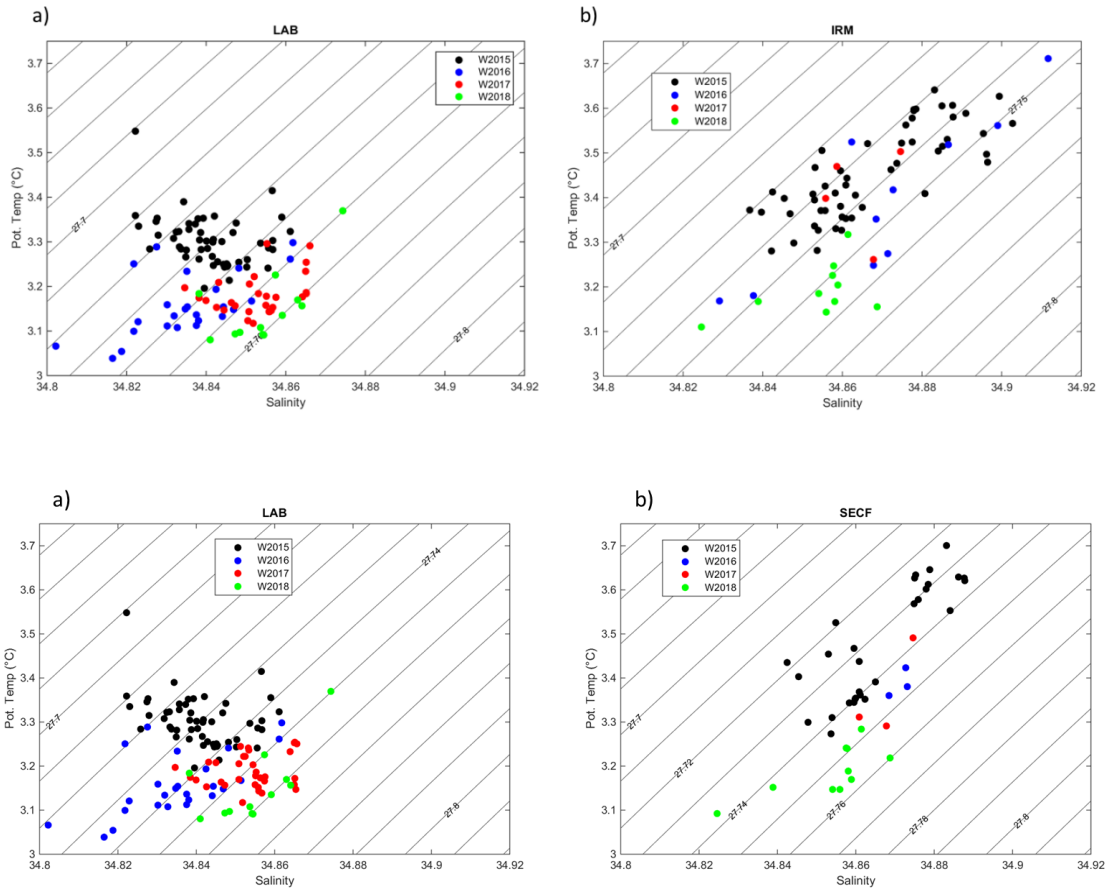

Figure 3. TS diagrams in the mixed layer for profiles with MLD deeper than 700 m during winters 2015, 2016, 2017 and 2018 for a) the Labrador Sea and b) SECF. The properties of the mixed layers were estimated as the vertical means between 200 m and the MLD. ~~Diagram TS of the n profiles with MLD deeper than 700 m found a) in the Labrador Sea and b) in Irminger Sea, in the winters 2015, 2016, 2017 and 2018. The properties of each profile were estimated as the vertical mean between 200 m and the MLD.~~

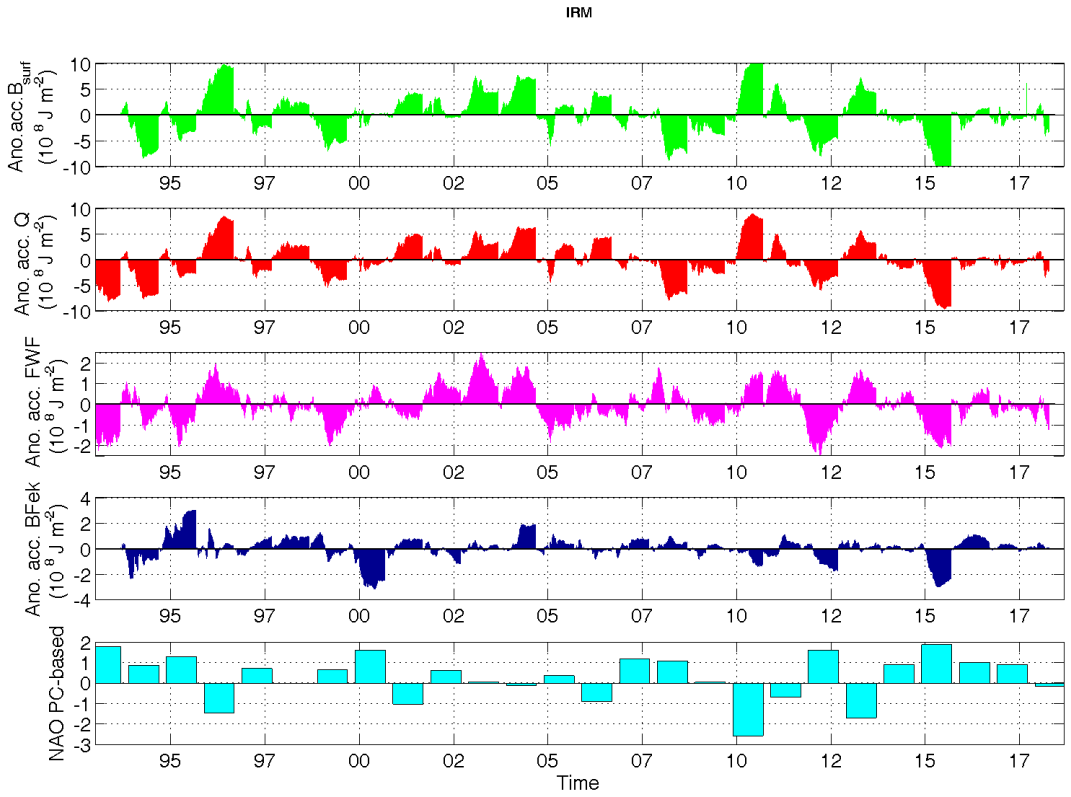
IRM
Ano.acc.B$_{surf}$ (10^8 J m^{-2})
Ano. acc. Q (10^8 J m^{-2})
Ano. acc. FWF (10^8 J m^{-2})
Ano. acc. BFek (10^8 J m^{-2})
NAO PC-based
95 97 00 02 05 07 10 12 15 17
Time

768

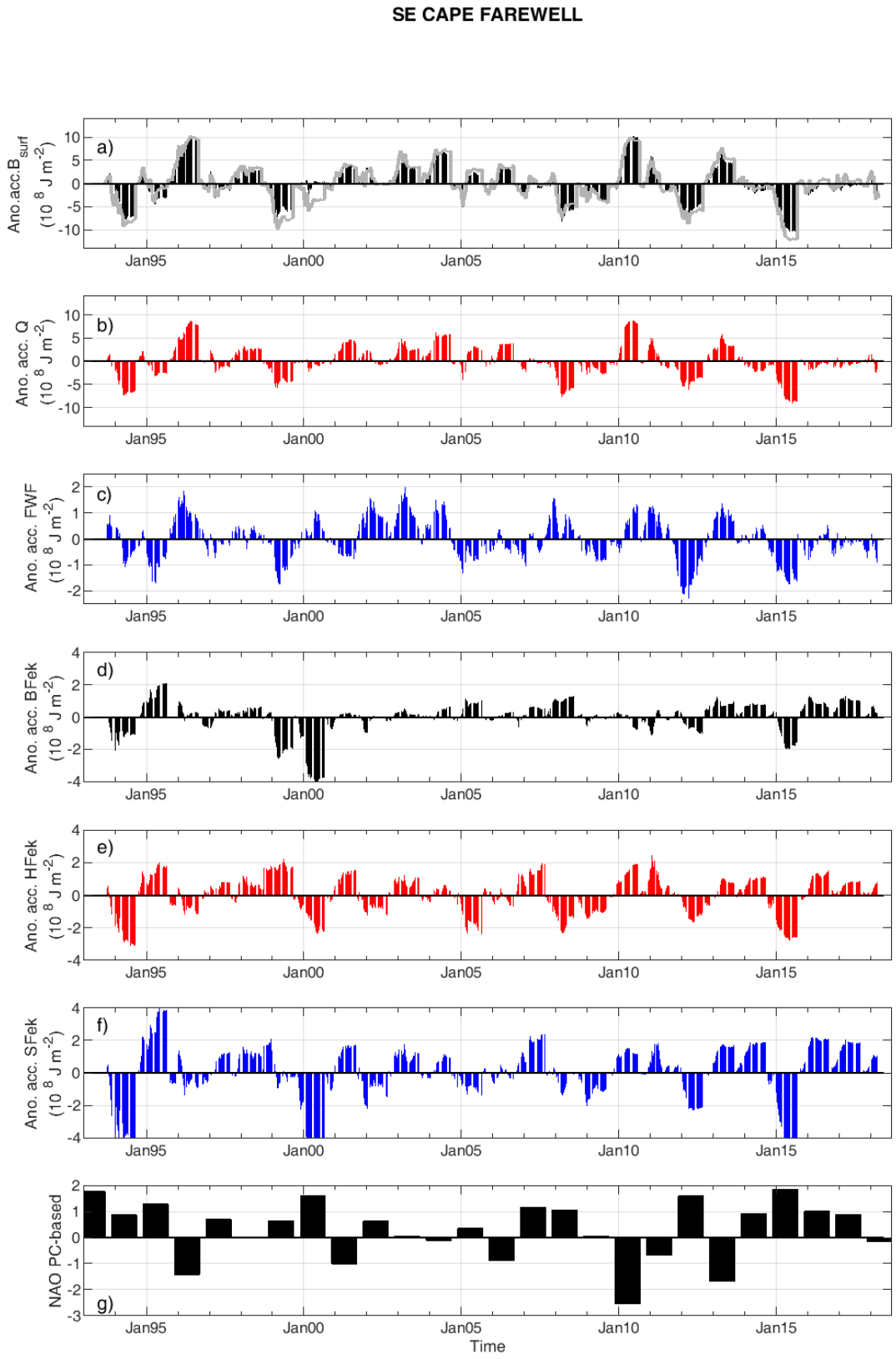

Figure 4. Time series of anomalies of accumulated a) Bsurf*, b) Q, c) FWF* d) BF_{ek}, e) HF_{ek} and f) SF_{ek}.

771 averaged in the SECF region.~~Bsurf*, Q, FWF* and BF_{ek}, averaged in the Irminger Sea.~~ They are
772 anomalies with respect to 1993 – 2016. The accumulation was from 1 September to 31 August the
773 following year. The winter NAO index (Hurrel et al., 2018) is also represented in ~~the bottom panel~~g).
774 Gray line in a) is the sum of the anomalies of accumulated B_{surf}* and BF_{ek}. Note that the range of
775 values in the y-axis is not the same in all the plots.

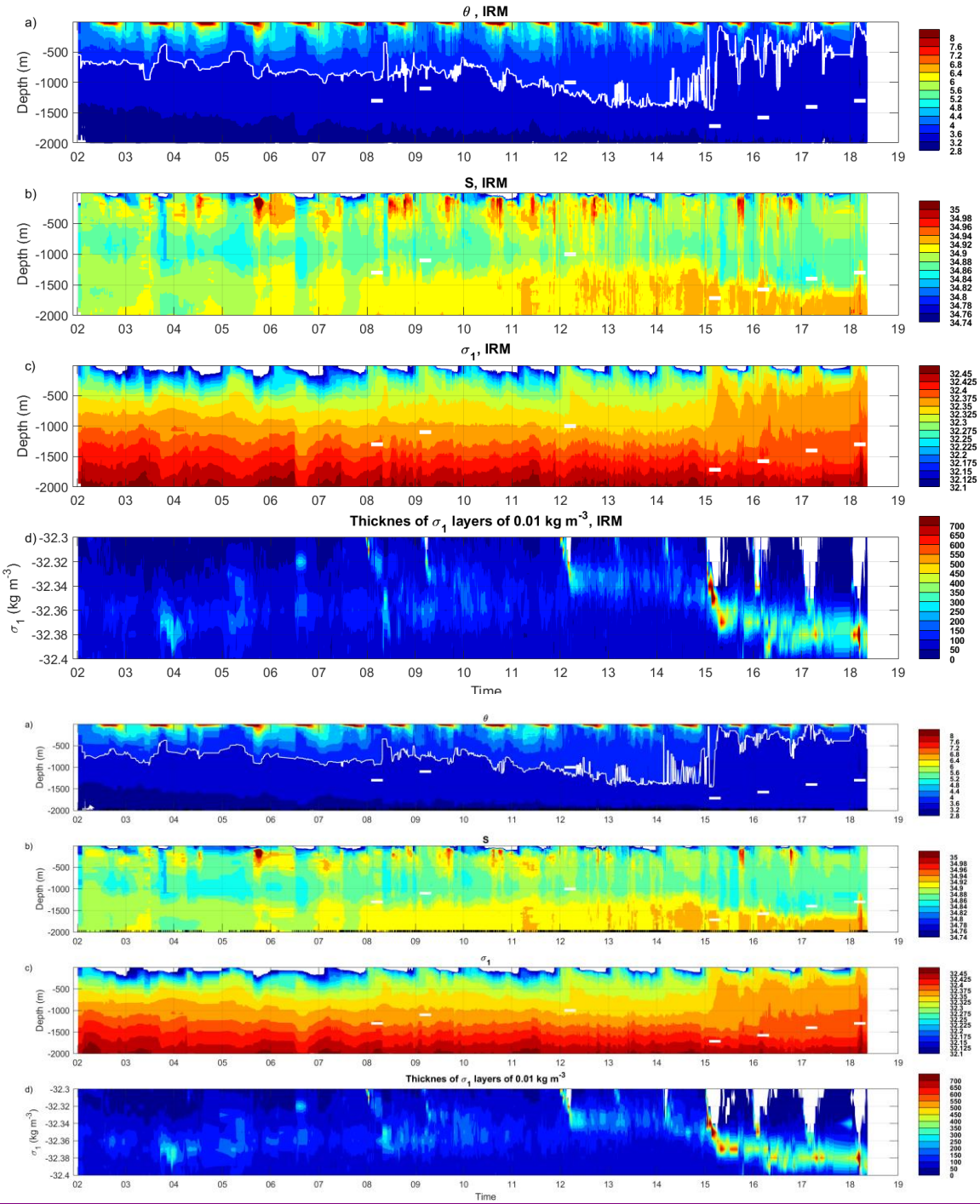

776

777

778 **Figure 5.** Time-evolution of vertical profiles measured from Argo floats in the ~~Irminger Sea~~SECF
779 region: a) θ ; b) S; c) σ_1 and d) thickness of 0.01 kg m^{-3} thick σ_1 layers. The white horizontal bars in

plots a), b) and c) indicate the maximal convection depth observed in the Irminger Sea or SECF when deep convection occurred. The white line in plot a) indicates the depth of the isotherm 3.6 °C. The black vertical ticks on the x-axes of plot b) indicate times of Argo measurements. These figures were created from all Argo profiles reaching deeper than 1000 m in the ~~IRM~~ SECF region (56.5° – ~~61~~59.3°N, 45°– 38°W, pink box in Fig. 1). The yearly numbers of Argo profiles used in this figure are shown in Fig. S5~~1~~.

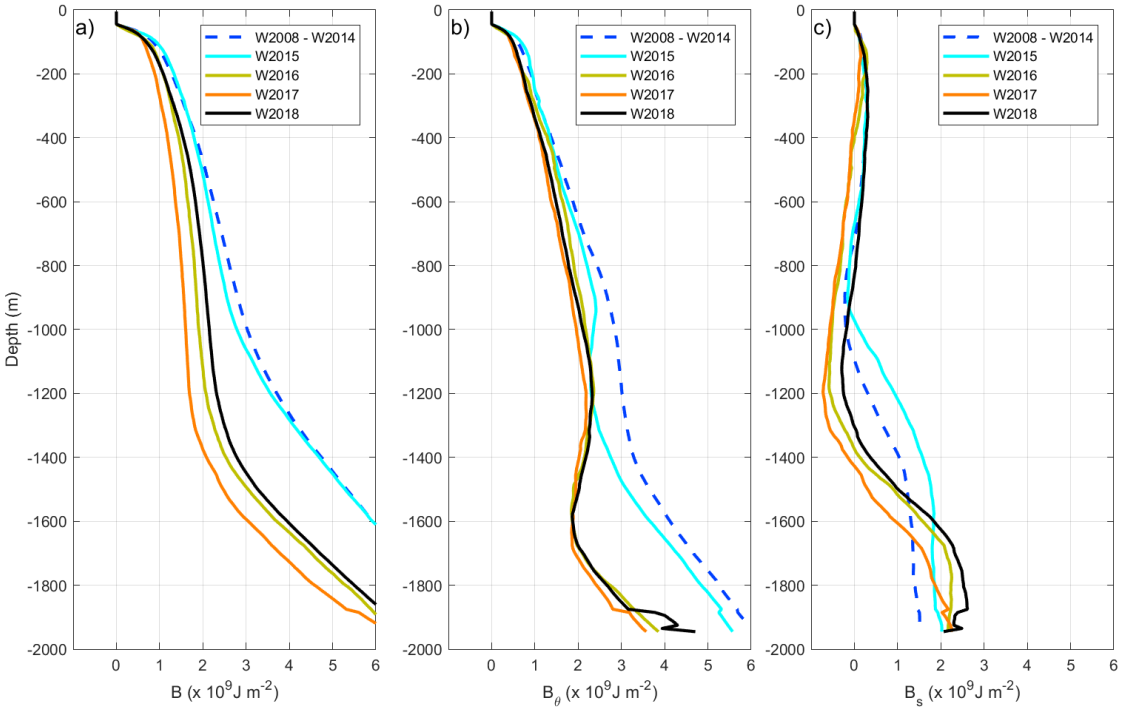

787

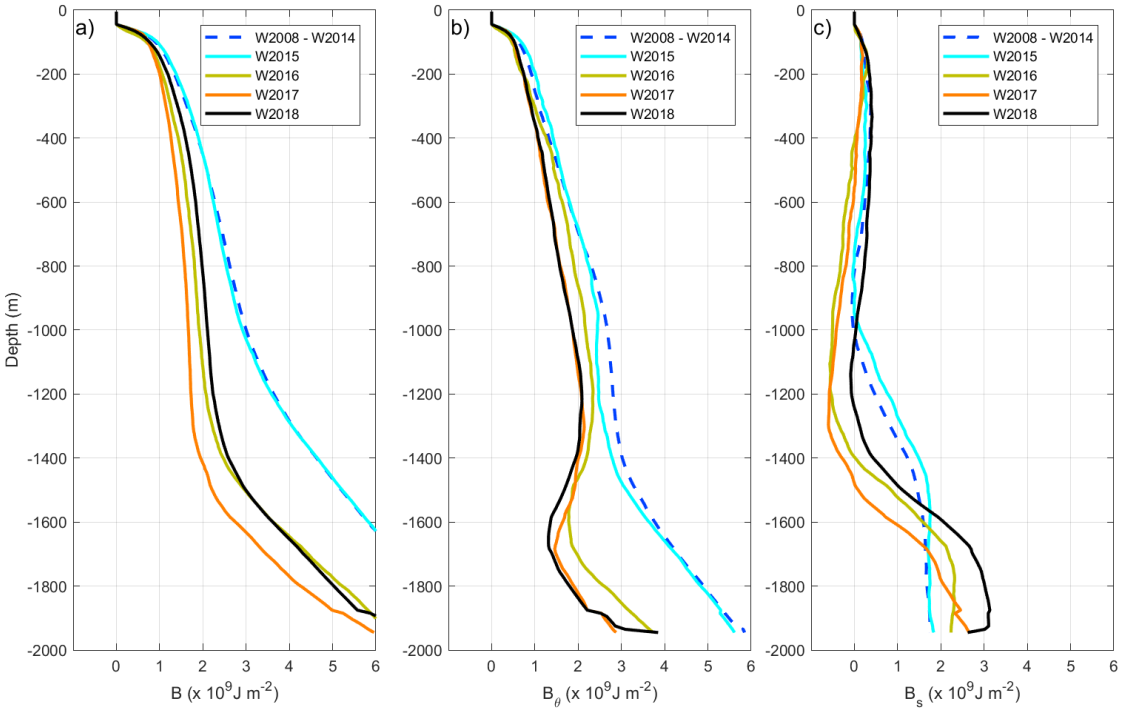

788

789 **Figure 6.** Vertical profile of a) the ~~total~~ buoyancy to be removed (B), b) the thermal component (B_θ)
790 and c) the salinity component (B_s). They were calculated from all Argo data measured in the ~~Irminger~~
791 SECF box (see Fig. 1) in September before the winter indicated in the legend. For W2015 and W2018,

we considered data from 15/08/2017 to 30/09/2017 because not enough data were available in September ~~2017~~. The number of Argo profiles taken into account to estimate the B profiles was more than ten for all the winters.

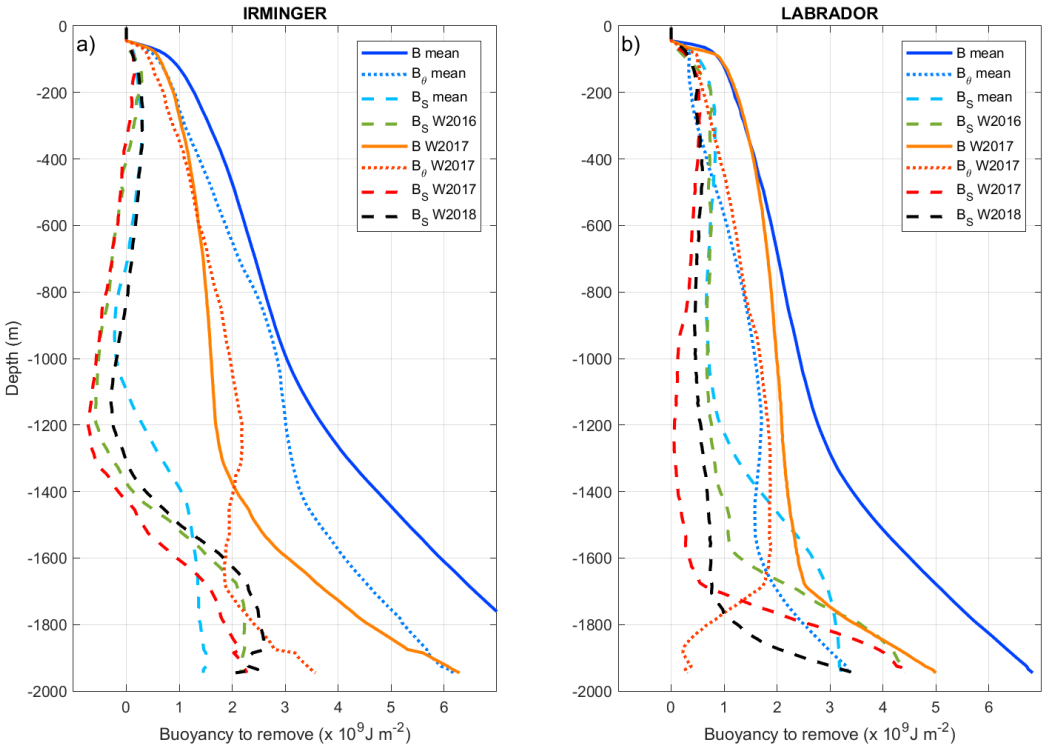

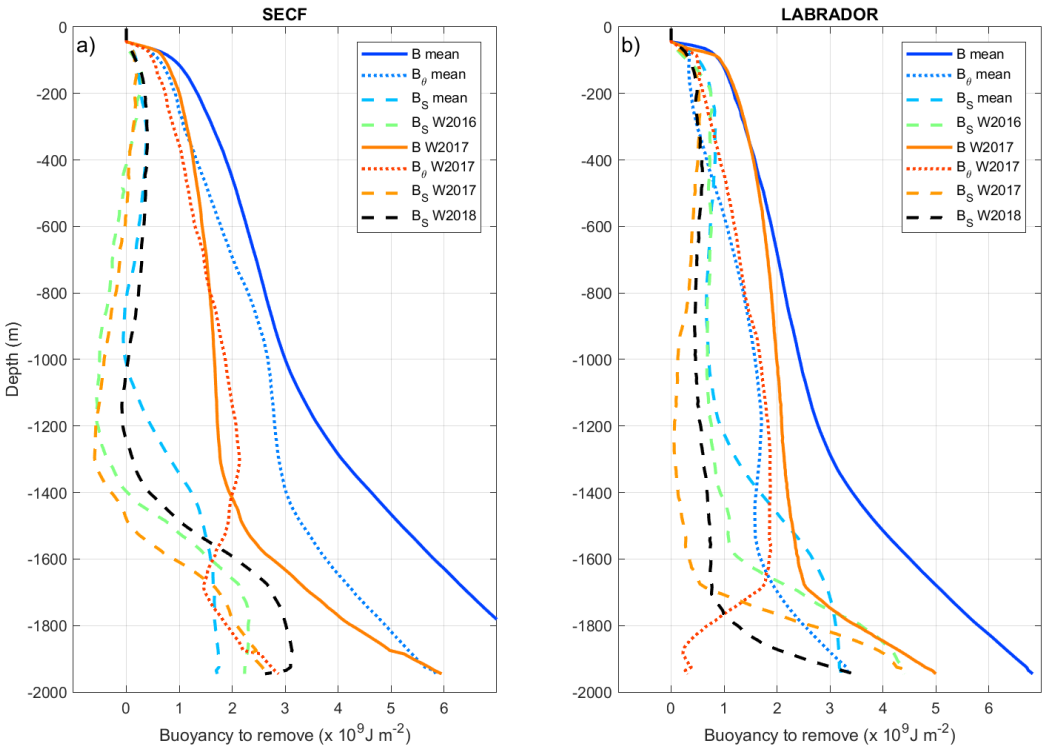

Figure 7. Decomposition of profiles of Buoyancy to be removed (B, continuous lines) in its thermal (B_θ, ~~point~~ dotted lines) and salinity (B_s, ~~discontinuous~~dashed lines) components in a) the ~~Irminger Sea~~SECF region; b) the Labrador Sea. ~~To compare the mean 2008 – 2014 with W2017 compare reddish lines with bluish lines.~~ The B_s component in W2016 and W2018 ~~was~~ were added ~~in order~~ to show the evolution of the depth of the deep halocline ~~in both the Irminger Sea and the Labrador Sea~~.

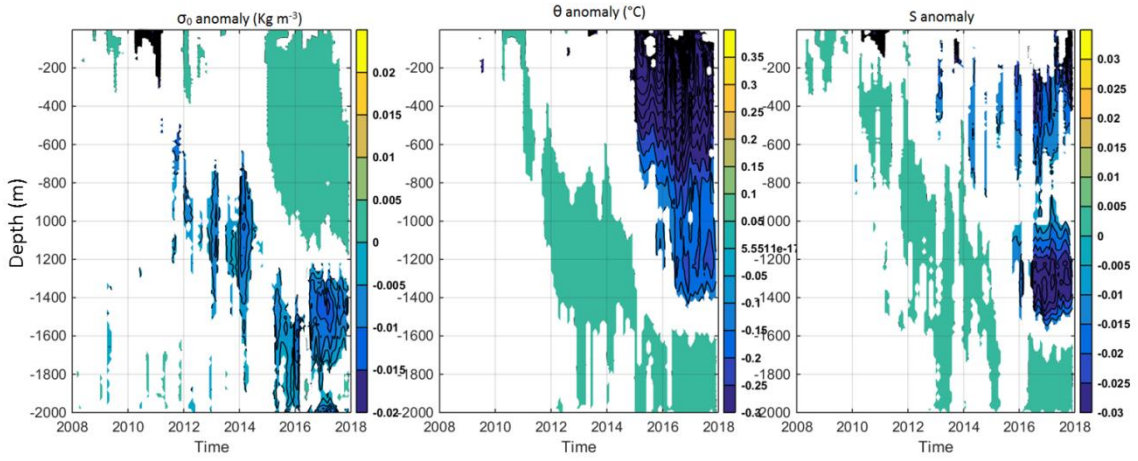

804

(58 °N - 40 °W)

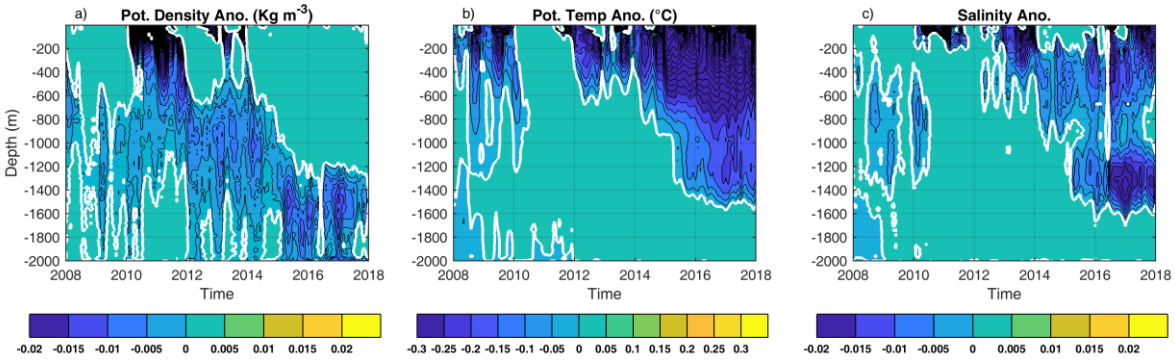

805

806 **Figure 8.** Evolution of vertical profiles of monthly anomalies of a) σ_0 ~~(left panel)~~, b) θ ~~(central panel)~~

807 and c) S ~~(right panel)~~, at ~~59~~58°N, 40°W ~~in the Irminger Sea~~. The anomalies were estimated from the

808 ISAS database (Gaillard et al., 2016), and they were referenced to the monthly mean estimated for

809 2002 – 2016. ~~We represented only anomalies larger than one standard deviation of the mean and~~

810 ~~since 2008 in order to see clearly the recent changes. All anomalies are displayed in Fig. S3.~~

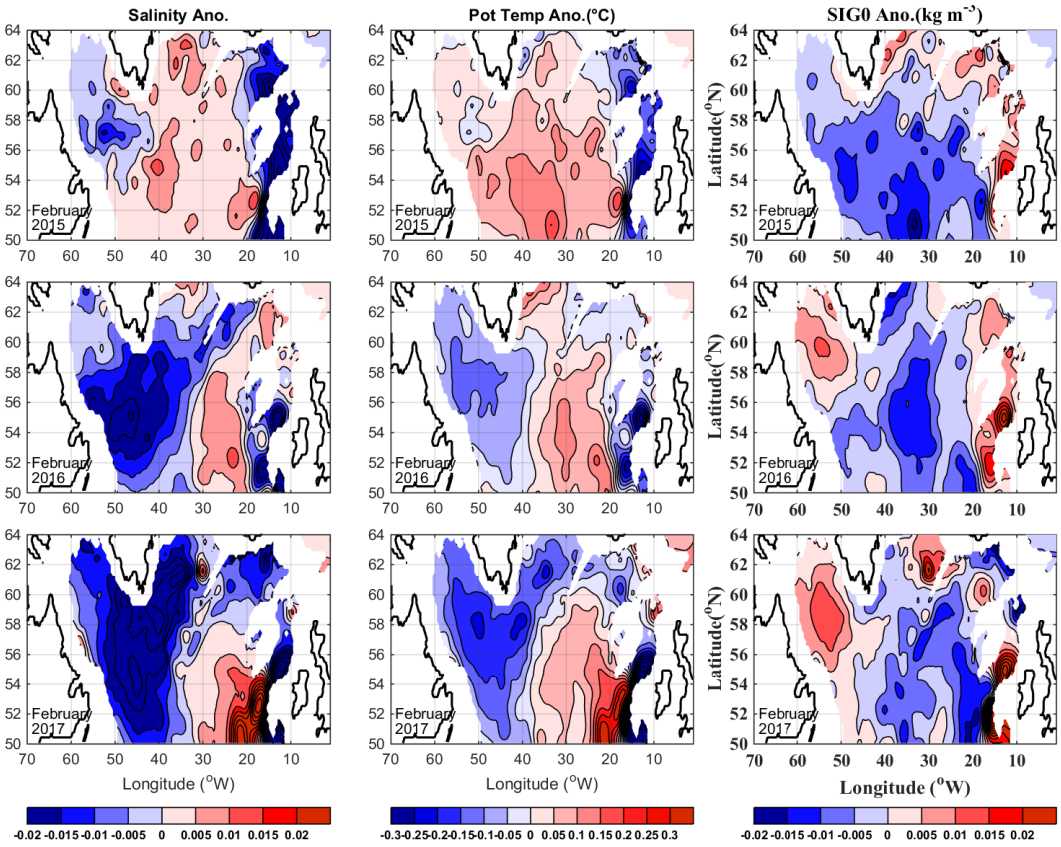

811

812 **Figure 9.** Horizontal distribution of the anomalies of S (left panels), θ (central panels) and σ_0 (right

813 panels) in the layer 1200 – 1400 m in February 2015 (upper panels), February 2016 (central panels)

814 and February 2017 (lower panels). The monthly anomalies were estimated from ISAS database

815 referenced to the period 2002 – 2016.

816

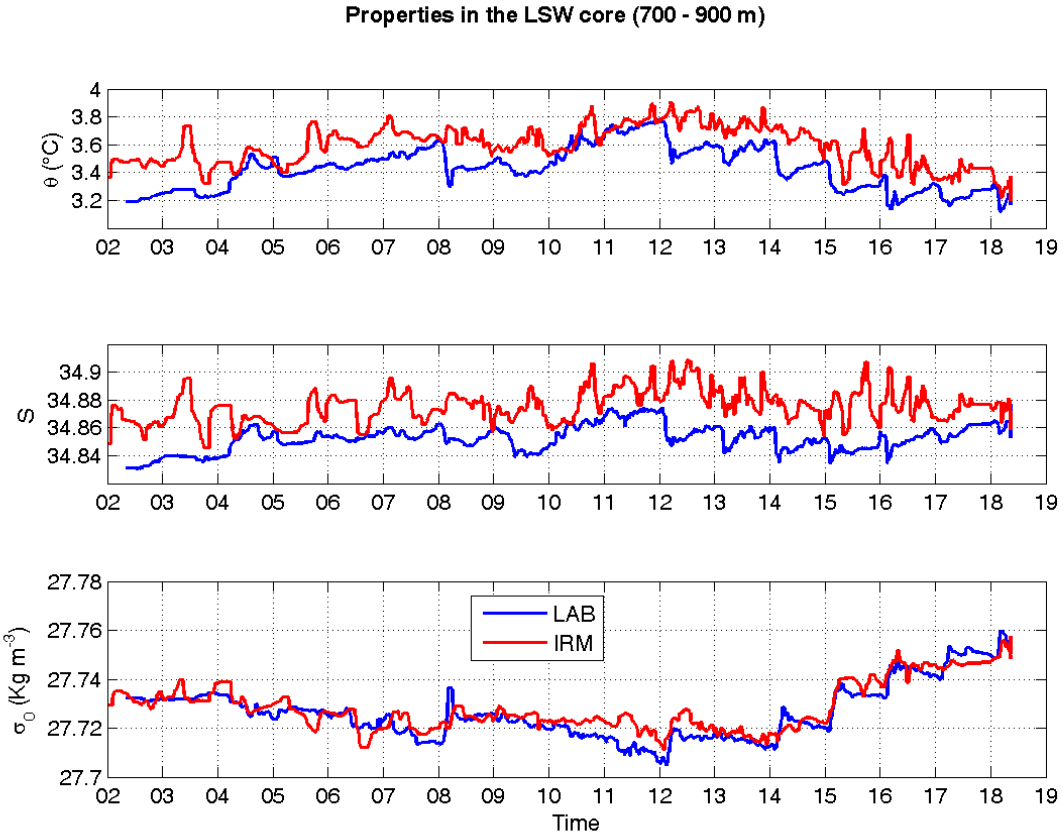

817

818 ~~Figure 10. Time evolution of the properties of the LSW core (700 – 900 m) in the Irminger Sea (red)~~

819 ~~and Labrador Sea (blue), estimated from all Argo data in the pink and cyan boxes in Fig. 1.~~

820

821

822

823

824

825